Evaluating novel compounds as radiosensitising agents



David Nderitu
St Cross College
University of Oxford

A Thesis submitted for the degree of **Master of Science (by Research) in Oncology**
Trinity 2024

Table of Contents

Abstract 4

Abbreviations, Acronyms and Definitions 7

Chapter 1: Introduction 9

1.1 Cancer 10

1.2 Radiotherapy and Radioresistance 10

1.3 Historical uses of Texaphyrin-Platinum (IV) conjugates as radiosensitising agents ... 14

1.4 Novel Texaphyrin-Platinum (IV) conjugate 21

1.5 DNA damage response 23

1.6 Shieldin: guardian of DNA ends and enemy of resection 27

1.7 DNA polymerase theta and its role in mediating DNA damage response pathways ... 28

1.8 DNA polymerase theta inhibitors as radiosensitising agents 30

1.9 Outline and purpose of the thesis 33

Chapter 2: Materials and Methods 34

2.1 Tissue Culture 35

2.2 Irradiation 36

2.3 Drugs and Solubility Testing 36

2.4 Cell viability assays 37

2.5 siRNA Transfection and Clonogenic Survival Assays 42

2.6 Immunoblotting 45

2.7 Statistical Analyses 48

Chapter 3: Results 49

3.1 MangaCisTEX fails to radiosensitise in H1299 and A549 cell lines 50

3.2 Cisplatin (IV) displays unexpected single-agent toxicity as a prodrug 53

3.3 MMn radioprotects in H1299 and A549 cancer models 55

3.4 Validation of SHLD2 KO cell line 58

3.5 Optimisation for the depletion of short-range resection factors using small- 59

interfering RNA 59

3.6 Depletion of short-range resection factors fails to abrogate the POLQi-mediated 61

radiosensitivity of SHLD2-disrupted 22RV1 cells 61

Chapter 4: Discussion 66

4.1 Summary of Findings I 67

4.2 Challenging the mechanisms of Texaphyrins and Platinum (IV) agents 67

4.3 Limitations of Project I 71

4.4 Conclusion and Future Perspectives I 72

4.5 Summary of Findings II 73

4.6a – Synthetic lethality of POLQ inhibition and 53BP1 defects 73
4.6b Short-resection and POLQi-mediated radiosensitisation..... 74
4.7 Limitations of Project II..... 76
4.8 Conclusion and Future Perspectives II..... 76
4.9 Concluding remarks..... 77
References: 78

Abstract

Radiotherapy is central to the curative management of cancer. A cell's lack of radiosensitivity is referred to as radioresistance, and it negatively affects patient outcome . The development and evaluation of radiosensitising agents is crucial for the improvement of RT efficacy. This project separately evaluated two radiosensitisers, MangaCisTEX and ART558.

MangaCisTEX is a chemical conjugate of the novel texaphyrin MMn and the inactive prodrug cisplatin (IV). This compound is thought to radiosensitise through the MMn-mediated reduction of a non-toxic cisplatin (IV) to the cytotoxic cisplatin (II).

SHLD2 is a commonly deleted gene in prostate cancers. We have previously observed that SHLD2-disrupted cells are sensitive to treatment with POLQi and RT. The POLQi-mediated radiosensitivity is hypothesised to be due to DNA end-resection. Consequently, we deplete shortrange resection factors, MRE11 and CtIP to see if this reverses or "rescues" radiosensitisation.

Our experimental aims were.

1. To characterise the radiosensitising effect of MangaCisTEX using *in vitro* lung cancer models
2. Understand the axis between POLQi-mediated radiosensitivity and DNA end resection in a SHLD2-disrupted model.

MangaCisTEX's radiosensitising effect was investigated using a cell viability assay in two lung cancer cell lines (n=3). We concluded that MangaCisTEX demonstrated strong cytotoxicity independent of radiation in both models. When analysing the individual moieties, MMn was found to have a radioprotective effect and cisplatin (IV) exhibited some cytotoxicity as an inactive prodrug. Against our hypothesis, MangaCisTEX failed to radiosensitise lung cancer cell lines.

The SHLD2-resection axis was investigated via colony formation assay in 22RV1 (prostate adenocarcinoma) WT and SHLD2 KO cell lines (n=3). At 4 μM POLQi it was concluded that neither the depletion of MRE11 or CtIP caused an abrogation of POLQi-mediated radiosensitivity. This indicated MRE11 and CtIP are not necessary for the initiation of resection, proposing a possible backup resection factor that works in their absence.

In loving memory of Grace Muthoni Mungai

Acknowledgements

I would like to express my heartfelt gratitude to my primary supervisor, Professor Geoffrey Higgins, for the opportunity to complete my master's degree in his laboratory. It has been a great pleasure to work for him.

I am particularly thankful to my secondary supervisor, Dr. Gonzalo Rodriguez-Berriguete, for his invaluable insights, guidance, and unwavering support – not only within the scope of my project, but also in shaping my growth as a scientist. I want to give thanks to the Higgins group for their helpful discussions and input during my time here. With minimal laboratory experience at the start, I am deeply grateful to Mr Purusotha Thambiayah and Ms Rathi Puliyadi for their immense patience when teaching me the *in vitro* techniques that allowed me to complete this project. I would also like to thank the members of the Seymour group whose questionable sanity levels made the office a lively and enjoyable place to be.

The work of Project I would not have been possible without Dr Adam Sedgwick and the Chemistry Department for synthesizing the drugs and helping with solubility tests.

To Cynthia, Ethan, Joe and Kyle, thank you for keeping me sane through our many video conferences. I am also very thankful to my Aunty Betty and her family for their support throughout the year and for opening their home to me. To my mother, father and brother, your unwavering love and support have been my greatest strength—I wouldn't be here without you.

Finally, I give thanks to God, whose grace and mercy have given me life and carried me on this journey.

Abbreviations, Acronyms and Definitions

Abbreviation	Definition	Abbreviation	
5FU	5-Fluorouracil	MGd	Motexafin Gadolinium
ANOVA	Analysis of variance test	MMEJ	Microhomology-mediated end joining
ART558	DNA polymerase theta inhibitor made by Artios Pharma	MRE11	Meiotic recombination 11
ATM	Ataxia Telangiectasia Mutated	MRN	MRE11-Rad50-NBS1
ATCC	American Type Culture Collection	NADPH	Nicotinamide adenine dinucleotide phosphate
BRCA1/2	Breast Cancer gene ½	NBS1	Nibrin
BSA	Bovine Serum Albumin	NER	Nucleotide Excision Repair
Chk2	Checkpoint kinase 2	NHEJ	Non-Homologous End Joining
CO-FISH	Chromosome-orientation fluorescence *in situ* hybridization	NSCLC	Non-small cell lung cancer
CtIP	C-terminal-binding protein-interaction protein	NT	Non-targeting
DDR	DNA Damage Response	PE	Plating efficiency
D-loop	Displacement loop	POLQ	DNA polymerase theta
DMSO	Dimethyl sulfoxide	POLQi	DNA polymerase theta inhibitor
DMEM	Dulbecco's Modified Eagle Medium	REV7	Revertability protein 7
DNA	Deoxyribose Nucleic Acid	RNA	Ribonucleic acid
DNA2	DNA replication helicase 2	ROS	Reactive oxygen species
DSS1	26S proteasome complex subunit	RNS	Reactive nitrogen species
DTT	Dithiothreitol	RPA	Replication protein A
dsDNA	Double-strand DNA	RPMI	Roswell Park memorial institute 1640
ECL	Enhanced chemiluminescence	RPF	Radiopotentiation factor
EPR	Enhanced Permeability Retention	RIPA	Radioimmunoprecipitation buffer
EXO1	Exonuclease 1	RT	Radiotherapy
FBS	Foetal Bovine Serum	SD	Standard deviation
FdUMP	Fluorodeoxyuridylate	SHLD1/2/3	Shieldin subunit 1/2/3

FdUTP	Fluorodeoxyuridine triphosphate	siRNA	Small-interfering RNA
FUTP	Fluorouridine triphosphate	Sirt3	Sirtuin 3
Gy	Gray	S/G2/G1/M phase	Synthesis/ Gap 2/ Gap 1/ Mitosis
H2AX	H2A histone family member X	ssDNA	Single-strand DNA
HR	Homologous Recombination	TBST	Tris-buffered saline tween
HRP	Horseradish Peroxidase	TLS	Translesion synthesis
IC50	Half-maximal inhibitory concentration	TNFa	Tumour necrosis factor alpha
IL1	Interleukin 1	VEGF	Vascular endothelial growth factor
IL6	Interleukin 6	WBRT	Whole body radiation therapy
IR	Ionising Radiation	WT	Wild Type
Isce1	Intron-encoded endonuclease	SHLD2 KO	SHLD2 Knockout
kDa	Kilodalton		
LINACS	Linear Accelerator		
lig4	DNA ligase IV		
MMn	Manganese texaphyrin		

Chapter 1: Introduction

1.1 Cancer

Cancer remains the globe's second-highest cause of morbidity and mortality, and its incidence is projected to rise in forthcoming years. Cancer is a disease characterised by uncontrolled cell proliferation and the spread of cells with an abnormal phenotype (1). Cancer is an umbrella term for over 250 types of cancerous diseases, all of which have unique genetic and environmental factors driving their pathogenesis (2). As such, developing efficacious treatments remains a challenge in the field.

The work of Hanahan and Weinberg (figure 1.1.1) helpfully characterised ten hallmarks of cancer as well as two emerging hallmarks and two enabling characteristics. The hallmarks can act as a heuristic device for researchers to use when attempting to understand the various cancer diseases and develop novel strategies for treating patients.

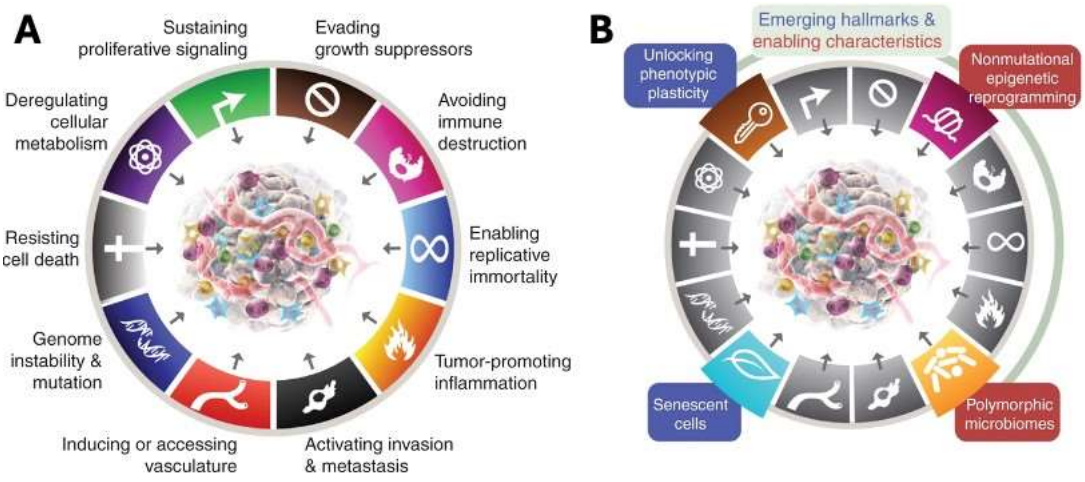

Figure 1.1.1 (A) Following the validation of two hallmarks, the six hallmarks of cancer originally described by Hanahan (2000) increased to eight hallmarks and two novel enabling characteristics in Hanahan (2011). (B) Recently, four more emerging hallmarks and enabling characteristics have been identified. This figure is from Hanahan et al. (2022).

1.2 Radiotherapy and Radioresistance

Radiotherapy (RT) is a central pillar of cancer therapy that is frequently used within the clinic. It is estimated that 50% of patients receive RT over the course of their illness (3). Approximately half of those patients receiving RT do so with curative intent, and this

treatment is administered as either a monotherapy or in combination with chemotherapy. A further 40% of patients receive RT treatment for palliative reasons, aiming to provide symptom relief and increase the quality of life for those with incurable disease (4,5). The other 10% of patients will receive RT for various other purposes, such as diagnostics or disease prevention (prophylactic). RT is administered by delivering varying dose rates of high-energy ionising radiation (IR) at tumour sites. The high energy IR can act directly on cellular DNA, causing vast DNA injury such as a DNA double-strand break (DNA DSB), which can be lethal, as well as DNA single-strand breaks (DNA SSB). IR also indirectly acts on cellular DNA via the generation of reactive oxygen/nitrogen species (ROS/RNS) secondary to the radiolysis of water, causing further DNA damage (6). RT is administered either externally or internally. External RT involves using linear accelerators (LINACS) to direct energy beams at the tumour site. Internal RT can be given using brachytherapy, where solid radioactive substances are administered into the body directly (7).

The efficacy of RT is defined as its ability to induce cancer cell death whilst sparing the surrounding normal tissue. However, tumours are heterogeneous by nature, and this makes control of the tumour and prediction of patient outcomes extremely difficult. The seminal work of Steel *et al.* revealed that the radiobiological effectiveness of RT is governed by five core principles, the 5 R's (8):

- Intrinsic **Radiosensitivity** of cells
- **Repair** of DNA damage
- **Reoxygenation** of hypoxic tumour regions
- Cancer cell **Repopulation** following a radiation dose
- **Redistribution** of cells within their cell cycle

By understanding these key radiobiological principles, scientists have been able to adapt RT treatment and improve its efficacy. A cell's intrinsic lack of radiosensitivity

(radioresistance) is often a large hindrance to RT treatment, becoming an indicator of poor patient prognosis and overall therapeutic failure. Radioresistance is a multifactorial phenomenon that can either be intrinsic to a cell or acquired by it (9,10). Intrinsic radioresistance is poorly understood, and we still lack a definitive mechanism for this phenomenon. The literature has posited a few mechanisms that may be involved, such as the role of sirtuin 3 (sirt3) in DNA damage response (DDR). Sirt3 is a class III histone deacetylase that is upregulated in cancers such as non-small cell lung carcinoma (NSCLC) (11,12). Sirt3 is believed to be an activator of the ATM-Chk2 pathway. The activation of this pathway increases the amount of G2/M arrest in the cell cycle, where more repair pathways, such as homologous recombination (HR) microhomology-mediated end joining (MMEJ) are ac,tive. This allows cells to repair DNA damage at a higher rate with more efficiency, meaning that these cells are intrinsically radioresistant (11). Additionally, there are some cases where the radioresistant phenotype can be acquired by tumours, and this is usually following some form of radiation induction. However, cases where the tumour acquires radioresistance do not tend to benefit from the effects of radiosensitising agents. Faced with the scenario where the very tumours that are being treated with RT have intrinsic radioresistance, the development of radiosensitising agents is crucial.

Over the years, many radiosensitising agents have gone through trials and made their way into clinical use. One example agent is the antimetabolite drug 5-fluorouracil (5-FU). 5-FU is a halogenated pyrimidine that exerts its sensitising effect through modulation of the cell cycle. During the S-phase of the cell cycle, 5-FU enters the cell, utilising the facilitated transport mechanism that uracil would use (13). Upon cell entry, it is converted into three metabolites: fluorodeoxyuridine monophosphate (FdUMP), fluorodeoxyuridine triphosphate (FdUTP) and fluorouridine triphosphate (FUTP). All three of these disturb RNA synthesis and the function of thymidylate synthase, which is involved in DNA synthesis (14). This disturbance of DNA/RNA synthesis hinders the repair of

radiationinduced DNA/RNA damage and promotes cell killing. 5-FU has seen the most clinical success as a radiosensitiser in the treatment of carcinoma uterine cervix and colorectal cancer (15).

5-FU has also demonstrated efficacy as a treatment for anal cancers when combined with another clinical radiosensitiser, Mitomycin C (16). Mitomycin C is an alkylating agent that forms crosslinks DNA at the adenine and guanine base pairs. Similar to 5-FU, it mainly acts to inhibit DNA synthesis, promoting cell killing as cells find it more difficult to recover from radiation-induced DNA damage (17). Platinum-based agents have also been used as radiosensitisers, specifically cisplatin. Cisplatin's chemotherapeutic mechanism of action stems from its ability to form covalent DNA adducts and intra/interstrand crosslinks (mechanism of action described in section 1.3). In a similar way to the aforementioned 5FU and Mitomycin C, cisplatin radiosensitises by inhibiting the cell's ability to repair radiation-induced damage. Additionally, taxanes are a class of chemotherapeutic agents that work by a slightly different mechanism, targeting the microtubule's activity in cell division. An example is paclitaxel, which has been used in clinics for the treatment of nonsmall cell lung cancer (NSCLC), eliciting their effect by binding to microtubules and stabilising them to make them non-dynamic, thus preventing their disassembly and stalling cell cycle progression (18).

The level of radioresistance varies between tumour types and can drastically affect patient outcomes. Therefore, it is vital to develop agents that sensitise tumour cells to the cytotoxic effects of RT and improve its efficacy. Developing radiosensitising agents is a balance between the evaluation of novel compounds, combining established radiosensitising agents or repurposing of pre-existing drugs already on the market for ease of clinical translation. These agents are key for improving patient outcomes when treated with RT. This thesis summarises the work of an MRes project split into two halves, separately evaluating MangaCisTEX and ART558 as radiosensitising agents. Therefore,

each section hereafter will have a subsection, Project I (in reference to MangaCisTEX) and Project II (POLQi).

INTRODUCTION I: MangaCisTEX

1.3 Historical uses of Texaphyrin-Platinum (IV) conjugates as radiosensitising agents

Texaphyrins are a branch of synthetically-designed macrocyclic compounds developed by Professor Jonathan Sessler from Texas University, Austin. The work of this group in developing texaphyrins led to the synthesis of MGd (19) (illustrated in Figure 1.3.1).

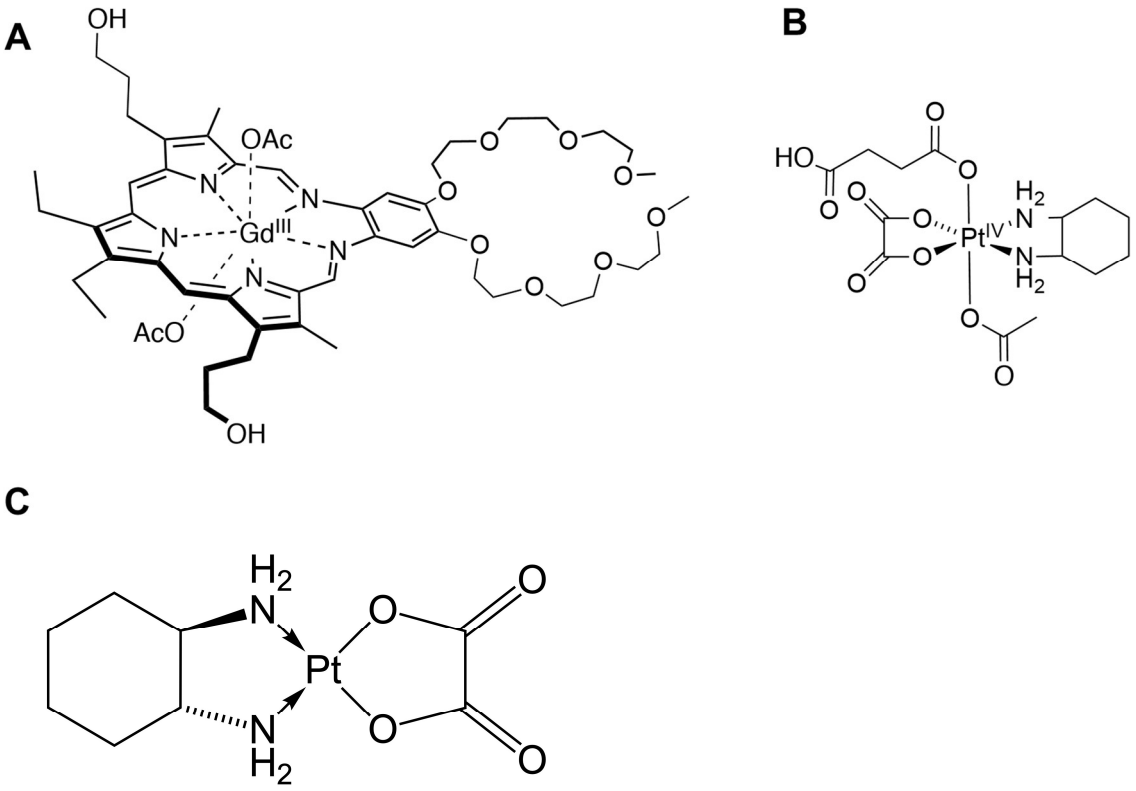

Figure 1.3.1 (A) The skeletal structure of MGd that has a strong affinity for electrons, contributing to its role as a redox-cycling agent. (B) The skeletal structure of an oxaliplatin (IV) prodrug is physiologically stable and inactive until reduced to its active form, oxaliplatin (II) (depicted in C). oxaliplatin (IV) offers more pharmacokinetic control by only exerting cytotoxic effects in a reducing environment.

MGd is a redox-active compound with high electron affinity, meaning that it is easily reduced by metabolites found in the cell, such as ascorbic acid and NADPH. From this reduction, an electron is donated to molecular oxygen in the cell, generating ROS species

like hydrogen peroxide and superoxide. However, during this process, the loss of this electron returns MGd to its original oxidised form. This process repeats on a loop, hence the term futile redox cycling. The effect of this on the cell is the relentless generation of ROS, putting the cell under constant oxidative stress. When this was discovered, it gave rise to a novel method of sensitising tumour cells (illustrated in Figure 1.3.2) (20). This warranted the investigation of how MGd's redox cycling can make it a good radiosensitiser for use in clinical practice.

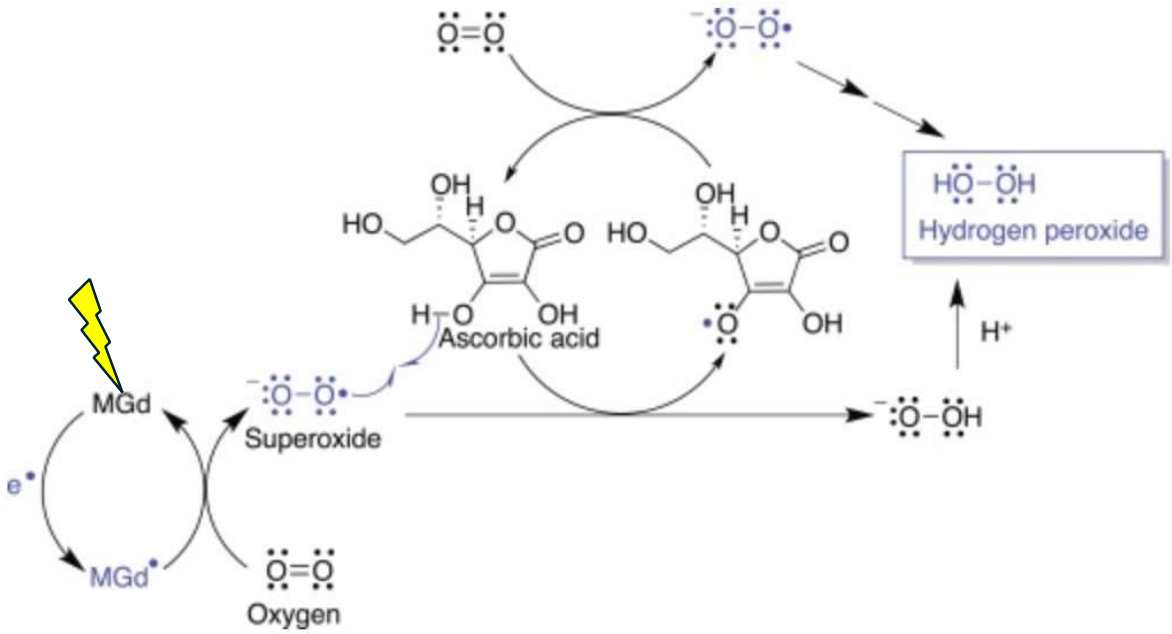

Figure 1.3.2 A schematic depicting how MGd acts as an electrophile in the presence of radiation. Its electrophilic activity potentiates the effect of radiation therapy by producing ROS species such as Hydrogen peroxide and Superoxide. The figure is adapted from Avendaño et al. (2023).

Secondary to MGd's redox cycling ability, the size of this macrocyclic molecule subject it to the ubiquitous pathophysiological phenomenon known as the enhanced permeability and retention (EPR) effect. The EPR effect arises due to the presence of three characteristics within solid tumours (21):

1. Increased neovascularisation
2. Increased expression of inflammatory cytokines
3. Decreased efficiency of lymphatic drainage

Tumour angiogenesis is often the reason tumours remain starved for nutrients and oxygen, as the new tumour vessels often have large fenestrations, making them leaky and abnormal (22). MGd is a large molecule (Molecular weight – 740.6 kDa) and these vascular fenestrations allow it to extravasate from the bloodstream into the tumour interstitium due to reduced vasculature integrity. The increased expression of proinflammatory cytokines such as IL-1, IL-6 and TNF-a lead to the sustenance of this EPR effect by inducing the expression of VEGF (23). Finally, due to an impaired lymphatic drainage system, MGd cannot be efficiently expelled when taken up by the tumour (24).

The decision for MGd to be taken into clinical trials as a tumour radiosensitiser was essentially three-fold. Firstly, it has a high electron affinity, allowing MGd to induce oxidative stress within the cell in the presence of radiation, and the presence of gadolinium within the molecule made it easy to visualise with magnetic resonance imaging (MRI). Its detection by MRI makes it easy for clinicians to track the accumulation of MGd in the tumour. Additionally, due to the EPR effect, the drug can localise well within the tumour and remain there for extended periods.

In the early 21st century, MGd entered various clinical trials as a single agent, in combination with other therapeutics and in combination with RT. A phase III clinical trial assessed MGd as a radiosensitising agent when administered with whole brain radiotherapy (WBRT) as a potential treatment for NSCLC patients with brain metastases. The trial recruited 554 adults with NSCLC, and they were split into groups that received WBRT (30 Gy in 10 fractions) alone as well as WBRT with MGd 5 mg/kg received 2-5 hours before IR). The study's endpoints were the interval to neurological progression and survival (both progression-free and overall). The study concluded that no significant difference was observed between the groups receiving WBRT and WBRT+MGd (25).

This suggested that MGd was not an effective radiosensitiser. However, at this time, little work had been carried out to assess the additional clinical benefit of combining MGd with other chemotherapeutic agents in the presence of radiation to improve its radiosensitising capacity.

The platinum agents routinely used in the clinic, such as oxaliplatin, cisplatin and carboplatin, are all platinum (II) agents and are a mainstay of chemotherapeutic cancer treatment. They can also be adapted for use as radiosensitising agents, further aggravating radiation-induced- DNA damage in the cell (21). The use of platinum agents in the clinic has always been impeded by its dose-limiting toxicities, with patients often experiencing myelosuppression (carboplatin), nephrotoxicity (cisplatin), neurotoxicity (oxaliplatin) and laryngospasms (oxaliplatin), to name a few (26). The emergence of new platinum (II) agents has been very limited, but in recent years, platinum (IV) complexes have been developed.

Platinum (II) drugs like cisplatin and oxaliplatin are activated by aquation reactions. These compounds generally adopt the square planar geometry, only containing four coordinate bonds, making them more susceptible to increased ligand substitution (27) (illustrated in Figure 1.3.4). The chloride ligand (cisplatin) or oxalate ligand (oxaliplatin) are displaced by water molecules when they enter the cell, and these aquated structures have a higher affinity for DNA binding (28,29). When bound to DNA, cisplatin can cause both intrastrand crosslinks (accounting for 90% of the damage it causes) and interstrand crosslinks (accounting for 10% of the damage it causes) (30). These crosslinks occur due to the binding of platinum to the N7 active site of purine base pairs. Most commonly, the aquated-platinum will bind to the active site of adjacent purine base pairs, forming 1,2-intrastrand crosslinks, but in other cases, platinum can bind to the active site of the guanine on opposing strands, causing an interstrand crosslink (ICL)(31). ICLs tend to be more deleterious as the adduct prevents DNA strand separation required for cell cycle

progression, often causing arrest in the late stages of S/G2 phases (illustrated in Figure 1.3.3) (32). Whilst intrastrand crosslinks are simpler and can be fixed by nucleotide excision repair (NER), ICLs are more complex, requiring repair by HR or the Fanconi anaemia repair pathway (33).

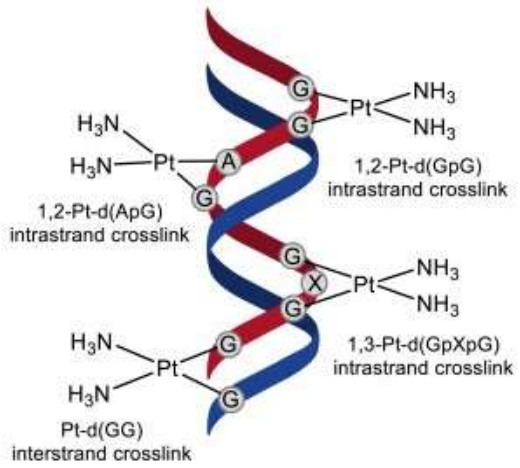

Figure 1.3.3 A schematic diagram illustrating the types of intrastrand and interstrand crosslinks that cisplatin can cause when bound to purinic base pairs. This figure is from Wang et al. (2018).

The platinum (IV) differ from the platinum (II) compounds as they adopt an octahedral geometry containing six-coordinate bonds, making their likelihood of premature ligand substitution much lower (34,35) (illustrated in Figure 1.3.4). Platinum (IV) complexes only then exert their cytotoxic activity once they come into contact with a reducing agent such as MGd, allowing them to adopt the square planar shape of platinum (II) complexes and increase the likelihood of ligand substitution and, therefore, allow the complex to exert cytotoxic effects. When existing in the platinum (IV) conformation, this drug should theoretically remain inactive and not cytotoxic.

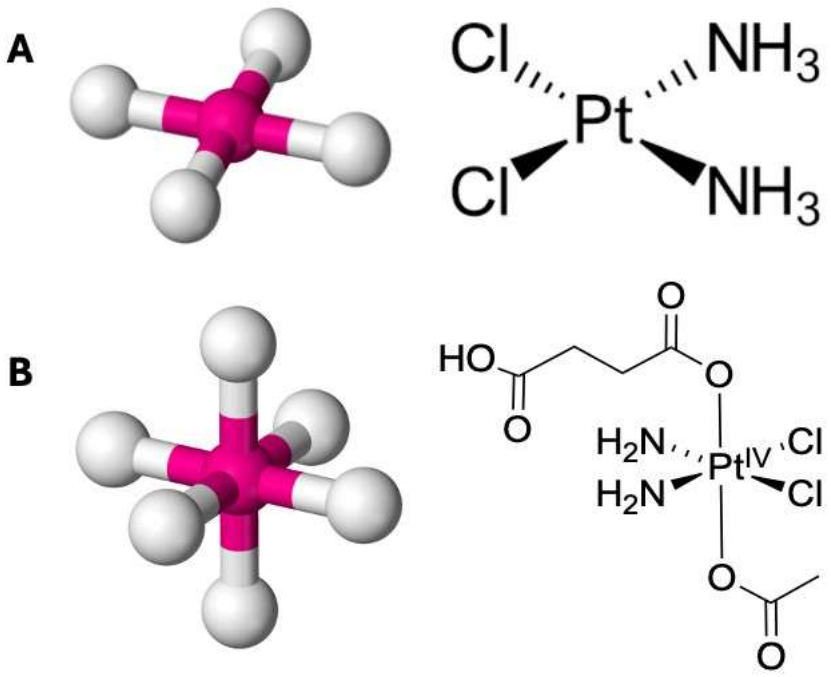

Figure 1.3.4 Schematic images depicting the coordinate geometry of platinum complexes where a platinum core (pink) is surrounded by axial ligands (white). (A) Cisplatin (II) adopts a square planar conformation. (B) Cisplatin (IV) adopts an octahedral conformation.

Arambula *et al.* significantly progressed the field by developing a Texaphyrin-Platinum (IV) conjugate (36,37). This aimed to provide proof of concept that this conjugate would allow for the tumour-specific delivery (via the texaphyrin) of a platinum (IV) payload, which is then reduced to platinum (II) exerting radiosensitising effects. Thus, overcoming the adverse effects associated with platinum treatment and allowing for improved tumourspecific radiosensitisation when compared to MGd alone. To ensure that the sensitising effect of both drugs would be seen without the premature reduction of the platinum (IV) agent, the texaphyrin was chemically conjugated to the agent as a caging method. When MGd was chemically conjugated to oxaliplatin (IV), this produced a compound called OxaliTEX. The research group performed Alexa Fluor 488 Annexin V staining to quantify both the amount of apoptosis and the moiety that caused it. They then compared the percentage signal for oxaliplatin (II), OxaliTEX and MGd (results shown in Figure 1.3.3).

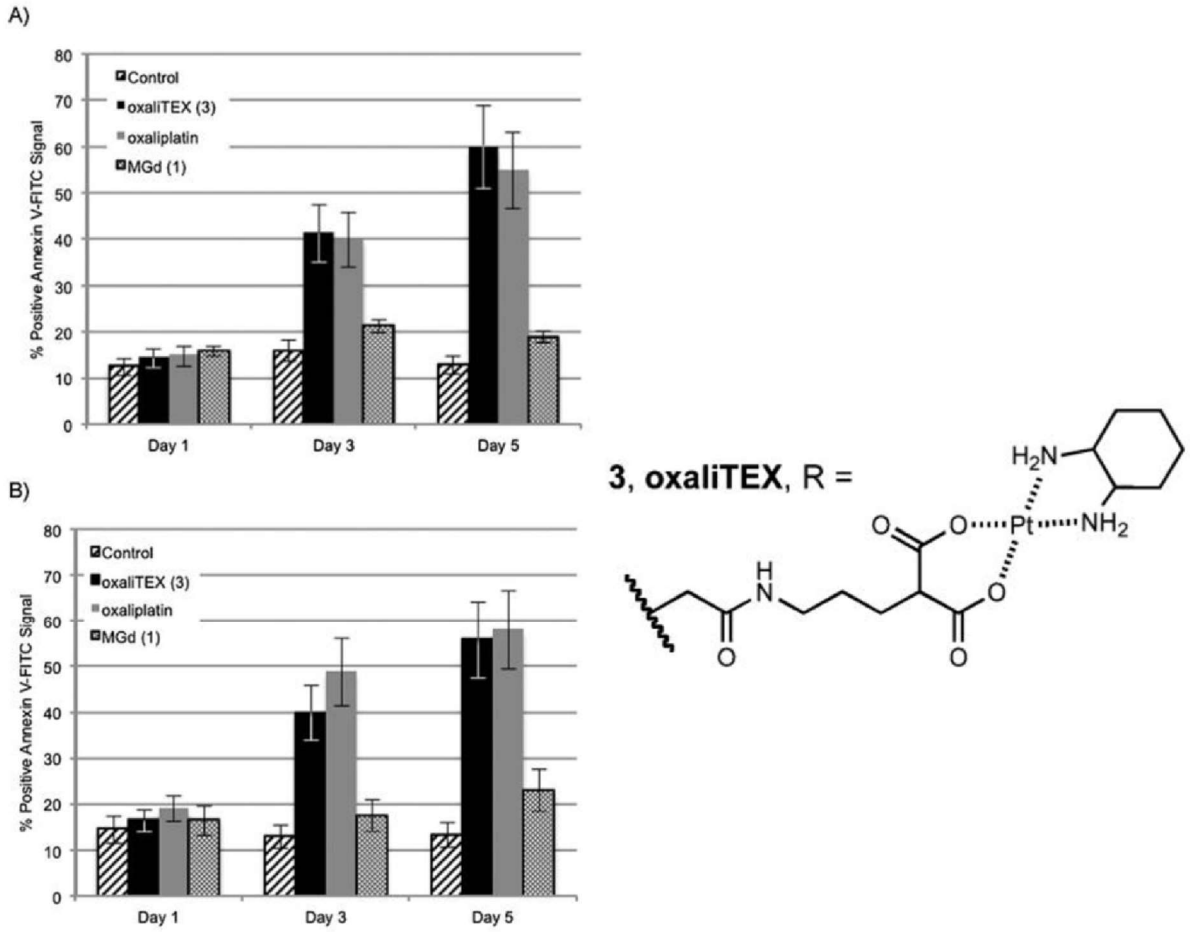

Figure 1.3.5 Representative images showing the percentage of apoptosis caused by OxaliTEX, oxaliplatin and MGd in (A) A2780 and (B) 2780CP cells and the structure of OxaliTEX. This figure is adapted from Arambula et al. (2012).

The results of this work indicated that the MGd-Oxaliplatin (IV) conjugate known as OxaliTEX was able to induce the largest percentage of annexin-V positive cells after three days. The data shows that the levels of apoptosis in cells exposed to OxaliTEX were nearly three times greater than those that were just exposed to MGd. The staining protocol also revealed which moiety of the conjugate was causing the most cell death. The radiosensitising effect of OxaliTEX was mainly due to the platinum (IV) moiety, which is reduced and not the texaphyrin that is conjugated to it. Due to Mehta's phase III trial indicating MGd was not an effective radiosensitiser, it was promising to see that conjugating a platinum (IV) agent to it significantly increased the radiosensitising potential (25). Arambula's work now posited the theory of texaphyrins acting more as transporter molecules for the platinum (IV) moiety when the two are conjugated, before facilitating its

reduction to platinum (II). This shifted the focus of the field as it was now possible to achieve greater radiosensitisation with Texaphyrin-Platinum (IV) conjugates compared to texaphyrin treatment alone.

1.4 Novel Texaphyrin-Platinum (IV) conjugate

Whilst the development of OxaliTEX was clinically promising, cisplatin (II) remained the first-line chemotherapeutic agent used in the clinic (38). Furthermore, cisplatin (II) is used as a radiosensitiser in various cancer subtypes such as head and neck, cervical and lung. In contrast, oxaliplatin (II) is only combined with RT for the treatment of oesophageal cancer. It can also be used as a single agent in the treatment of colorectal cancers, but this is without radiation, as the abdomen cannot tolerate RT. Therefore, to ensure the Texaphyrin-Platinum (IV) conjugate would be translationally relevant, the possibility of an MGd-Cisplatin (IV) conjugate (CisTEX) was explored alongside the OxaliTEX experiments.

Arambula's group used A2780 cisplatin-sensitive cells to perform an MTT assay assessing the level of cell proliferation at increasing concentrations of CisTEX and OxaliTEX. On the fifth day, MTT was added to each well and absorbance values were measured and fitted to a sigmoidal dose-response curve. This allowed them to calculate an IC_{50}. CisTEX gave an IC_{50} of 1.63 μM compared to 0.55 μM in OxaliTEX (37).

Additionally, recent literature has come to light suggesting that a class of compounds known as gadolinium chelates (compounds where a ligand forms a coordinate bond to a metal ion) have been linked with inducing neuropathy and nephrogenic systemic fibrosis in patients through premature release of free Gd^{3+} (39). Although uncommon, this issue is especially pertinent for patients with renal problems, as this often leads to gadolinium retention and a larger probability of the patient experiencing adverse effects (40).

Furthermore, MGd had already failed a phase III clinical trial as it was unable to demonstrate a significant increase in survival (both overall and progression-free). Essentially leaving the field with a texaphyrin that was not effective as a single-agent radiosensitiser and demonstrated toxicity in a small subset of patients. Whilst MGd's radiosensitising capacity was shown to be augmented when conjugated to a platinum (IV) complex, MGd itself was proving a slightly problematic construct.

As a result of this, we looked into a compound developed by Dr Adam Sedgwick from King's College London (Formerly of Texas University, Austin), known as Motexafin manganese ($MMn(NO_3)$ - herein referred to as MMn). MMn is a novel Texaphyrin compound that has a proposed mechanism of action that is analogous to MGd. Structurally, the two compounds are nearly identical, with MMn having a Manganese (II) core as opposed to MGd's Gadolinium (III) core (structures are illustrated in Figure 1.4.1). The logic behind developing MMn was to minimise the risks associated with gadoliniumretention toxicity by increasing the Texaphyrin's chelating ability, and this was achieved using a core metal in a lower oxidation state. Both metals are toxic when found in excess, but unlike Gadolinium, Manganese is a biological trace element naturally found in the body, and as such, there are efflux transporter molecules such as SLC30A10 which act to regulate manganese levels and prevent toxicity.

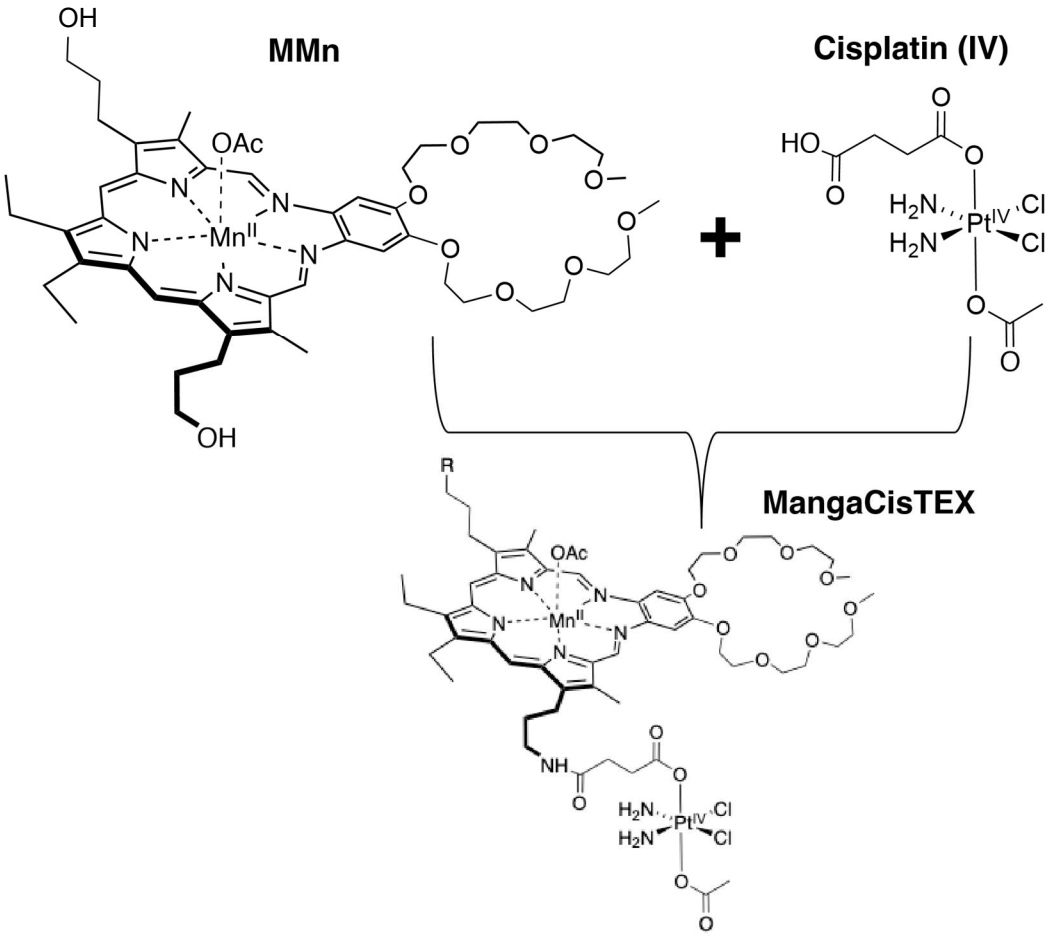

Figure 1.4.1 The molecular formula for MMn Texaphyrin, cisplatin (IV) prodrug and MangaCisTEX, the novel Texaphyrin-Cisplatin (IV) conjugate that is being evaluated as a novel tumour radiosensitising agent. The compound was developed from the work on the MGdoxaliplatin (IV) conjugate, oxaliTEX, that was synthesised in previous years.

MMn has the potential to radiosensitise more efficiently than MGd and may have its radiosensitising capacity augmented by conjugation with a platinum (IV) agent. MangaCisTEX is a novel MMn-Cisplatin (IV) conjugate with possible antitumour effects.

INTRODUCTION II: POLQi

1.5 DNA damage response

The integrity of the genome is essential for life, it keeps the cell proliferating and ensures that genetic information is passed on to the next generation. However, the cell is under a

constant state of genomic stress, from external causes such as ultraviolet (UV) radiation as well as the internal by-products of cellular processes such as ROS/RNS. DNA is constantly being damaged, and as a result, the DNA damage response (DDR) has been conserved throughout evolution. The DDR describes a cluster of enzymes and molecules that are involved in the sensing and repair of DNA damage. Conceptually, DDR can be categorised as a three-step mechanism (41).

1. Use of DNA sensors – to detect sites of DNA damage
2. Activation of DNA transducers/kinases – transduce signals to downstream effector molecules
3. DNA effectors – elicit a response of apoptosis, DNA repair, cell cycle arrest or senescence

The DDR's downstream signalling pathways essentially push the cell into programmed cell death, mitotic catastrophe or survival. Therefore, to fully gain control of various tumour types using radiation therapy, one must first understand radiation-induced DNA damage (RIDD) (42).

Canonically, DNA DSBs are repaired by one of two major repair pathways: nonhomologous end joining (NHEJ) or homologous recombination (HR). A third backup pathway exists for cases where there is excessive DNA-end resection revealing ssDNA (which can be caused by Ku70/80 or 53BP1 depletion) or the collapse of the replication fork, and this is known as microhomology-mediated end joining (MMEJ) (43). Of the three DSB repair pathways, HR is thought to have the highest fidelity as it uses regions of homology on identical sister chromatids. NHEJ is relatively error-prone as some frequent insertions/deletions may occur at the site of the break (44). However, MMEJ is considered the most error-prone due to the activity of translesion polymerases like POLQ used in the pathway. POLQ can extend DNA mismatched homologies as well as direct DNA extension without a template, often leading to high percentages of error in DNA repair (45,46). All

three pathways obey the three-step mechanism mentioned above, requiring the initiation step to be carried out by a DNA sensor complex.

The two major molecules involved in this initial step are the Mre11/Rad50/NBS1 complex (MRN) and gH2AX. The earliest stage of DDR is the recruitment of inactive MRN by RAD17 and MRN interacting protein (MRNIP) (47). This initiation step facilitates the loading of MRN onto the chromatin whilst causing ataxia telangiectasia mutated (ATM) to localise at the site of the damage. ATM acts to phosphorylate the Ser-139 residue of H2AX, allowing the protein to become activated and interact with the NBS1 region of the MRN complex, further recruiting more MRN to the site of DNA damage (48). DNA DSB repair is cell-cycle-dependent therefore, MRN can only become endonucelolytically active to perform end resection in the synthesis (S)/Gap 2 (G2) phases of the cell cycle, where DNA integrity is checked before mitosis. However, MRN's activity in the Gap 1 (G1) phase, where NHEJ dominates, is for DNA end tethering as opposed to end processing, allowing downstream ligation to occur (49). MRN activation is reliant on CtIP, the CtBP (carboxy-terminal binding protein) interacting protein. When bound to retinoblastoma protein (Rb), CtIP releases transcription factors that increase the expression of genes required for cell progression into the S phase (50). Following this, CtIP is phosphorylated in a cyclin-CDK-dependent manner, allowing the protein to localise to MRN and form an endonucelolytically active protein complex (51).

At the site of damage, the MRN-CtIP complex creates an endonuclease-nick on the 5' strand before performing short-range resection utilising MRE11's 3'-5' exonuclease activity. The initial short-range resection performed by MRN-CtIP results in the generation of short tracts of 3' single-stranded DNA (ssDNA) (52). The initial short-range resection step is essential for starting HR and MMEJ in the S/G2 phase of the cell cycle. Whilst all three repair mechanisms are initiated by the action of MRN, only HR and MMEJ utilise

MRN's endonucleolytic end processing. HR goes one step further, also utilising exonuclease 1 (EXO1) and DNA2/BLM as long-range resection factors. These long-range resection factors are recruited to the short 3'-tracts of ssDNA, and through the 5'-3' dsDNA exonuclease activity of EXO1, the ssDNA overhang is extended (53). As the 3'ssDNA overhang is extended, this provides a better template for replication protein A (RPA) to bind and protect the exposed ssDNA from nucleolytic degradation. RPA is then switched for Rad51 in a BRCA2-DSS1-dependent manner, and Rad51 mediates ssDNA strand invasion into neighbouring sister chromatids at regions of homology (54). This leads to the formation of a D-loop where the ssDNA can then be repaired back into the original dsDNA (illustrated in Figure 1.5.1). HR is a repair mechanism with high fidelity that competes with NHEJ for the repair of DSBs. However, it is established that approximately 80% of all DNA DSBs will be repaired by NHEJ as HR requires the presence of a sister chromatid and is only active in S/G2 (55).

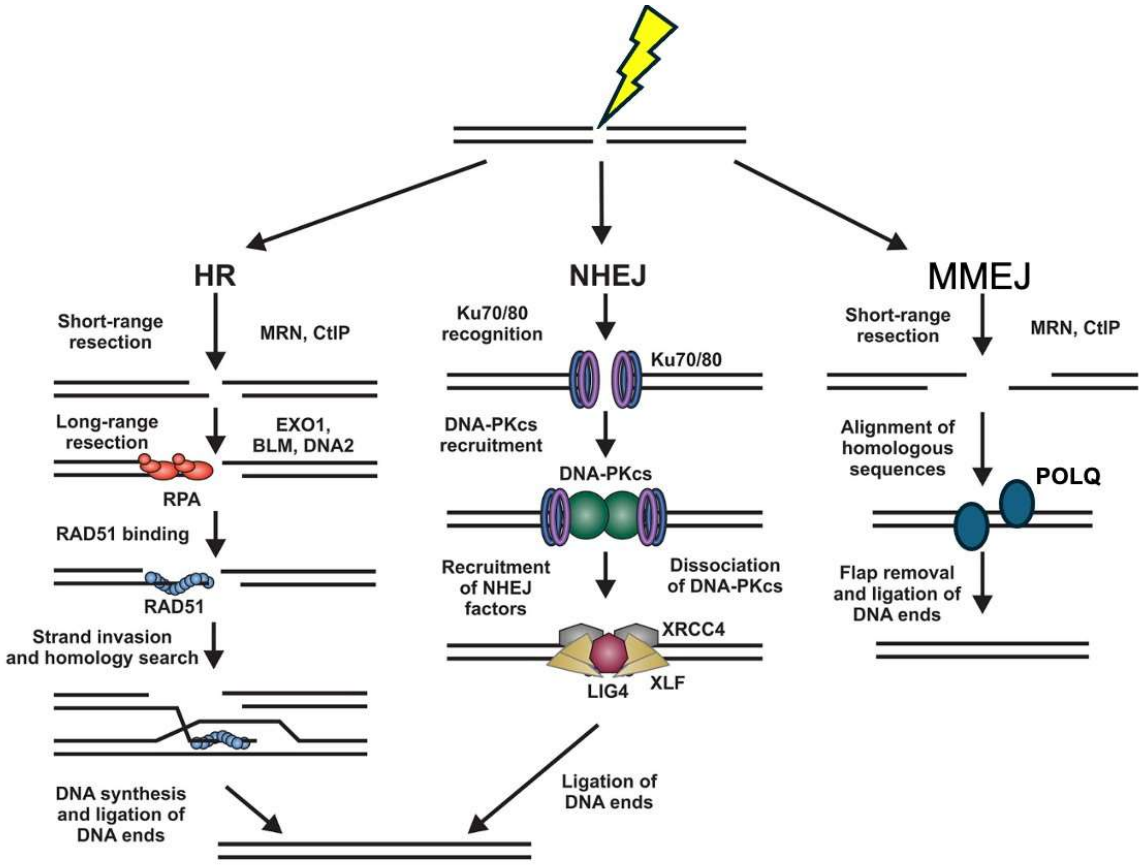

Figure 1.5.1 Schematic diagram illustrating the three canonical pathways that could be used to repair a DNA DSB. HR and NHEJ are the repair pathways with higher fidelity mainly used by the cell, and MMEJ acts as a backup. This figure is adapted from Ackerson et al. (2021).

1.6 Shieldin: guardian of DNA ends and enemy of resection

NHEJ is responsible for the majority of DNA DSB repair as it is not cell cycle-dependent like HR. The cell's decision to undergo resection-dependent (HR/MMEJ) or independent (NHEJ) repair is governed by 53BP1. The mechanism by which 53BP1 protects DNA ends through resection antagonism remains elusive, but evidence suggests this is carried out by the effector complex, shieldin (52). Shieldin is a four-subunit complex made up of C20orf196 (SHLD1), FAM35A (SHLD2), CTC-534A2.2 (SHLD3) and REV7.

Following the initial short-range resection initiated by MRN-CtIP, H2AX is activated by ATM via its interaction with NBS1. H2AX activation is essential for the recruitment of ubiquitin ligases, ring finger protein 8 (RNF8) and ringer finger protein 168 (RNF168). Together, these act to recruit p53 binding protein 1 (53BP1) and RIF1, forming an inactive complex. Activation of this complex causes shieldin to localise to the DSB in an ATMdependent manner (52). The shieldin complex binds to ssDNA via the three tandem OBfolds of the SHLD2 subunit and stops the extension of ssDNA by long-range resection factors such as EXO1 and DNA2/BLM. Once bound, shieldin recruits CTC1-STN1-TEN1 (CST) complex and its accessory enzyme polymerase-a to the site of the break, where polymerase-a will synthesise new DNA within the short ssDNA overhang (56). Finally, the DSB is repaired and joined by DNA ligase IV along with its accessory factors XRCC4/XLF (shown in Figure 1.6.1).

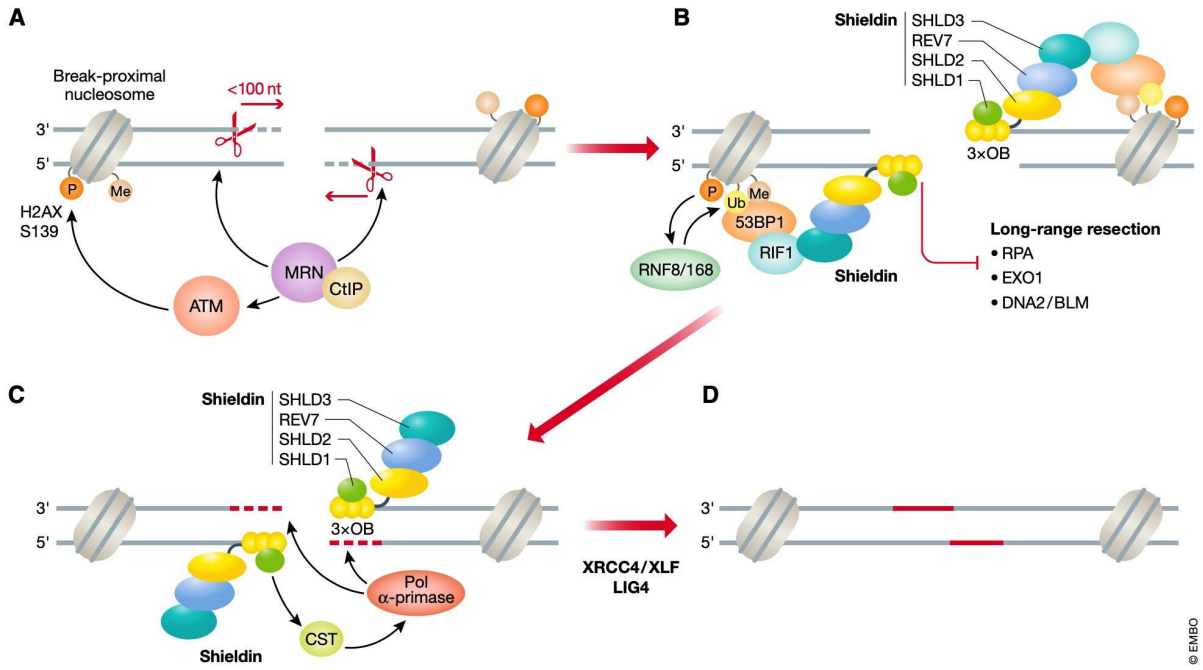

Figure 1.6.1 A schematic diagram indicating how the shieldin antagonises long-range resection within the cell, allowing DSB to be repaired by NHEJ whilst antagonising repair by HR. This figure is from Setiaputra et al. (2019).

According to the cancer genome atlas, there is an elevated incidence of SHLD2 deletion mutations in 6-13% of prostate cancer cases. A meta-analysis revealed that metastatic cases of prostate cancer have extremely low levels of SHLD2 mRNA expression (57). As a positive regulator of DNA DSB repair by NHEJ, SHLD2 deletion is thought to contribute to a hyper-resection phenotype within the cell, increasing the rate of breaks repaired by resection-dependent HR and MMEJ. Therefore, cells with SHLD2 deletions are particularly sensitive to DSB-inducing agents such as radiation as the rate of error in repair increases (58).

1.7 DNA polymerase theta and its role in mediating DNA damage response pathways

DNA polymerase θ (encoded by the POLQ gene) is a large, highly conserved protein found in mammals. The protein contains a helicase-like domain at its N-terminus, a disordered

central domain and a polymerase domain at the C-terminus (structure illustrated in Figure 1.7.1) (59).

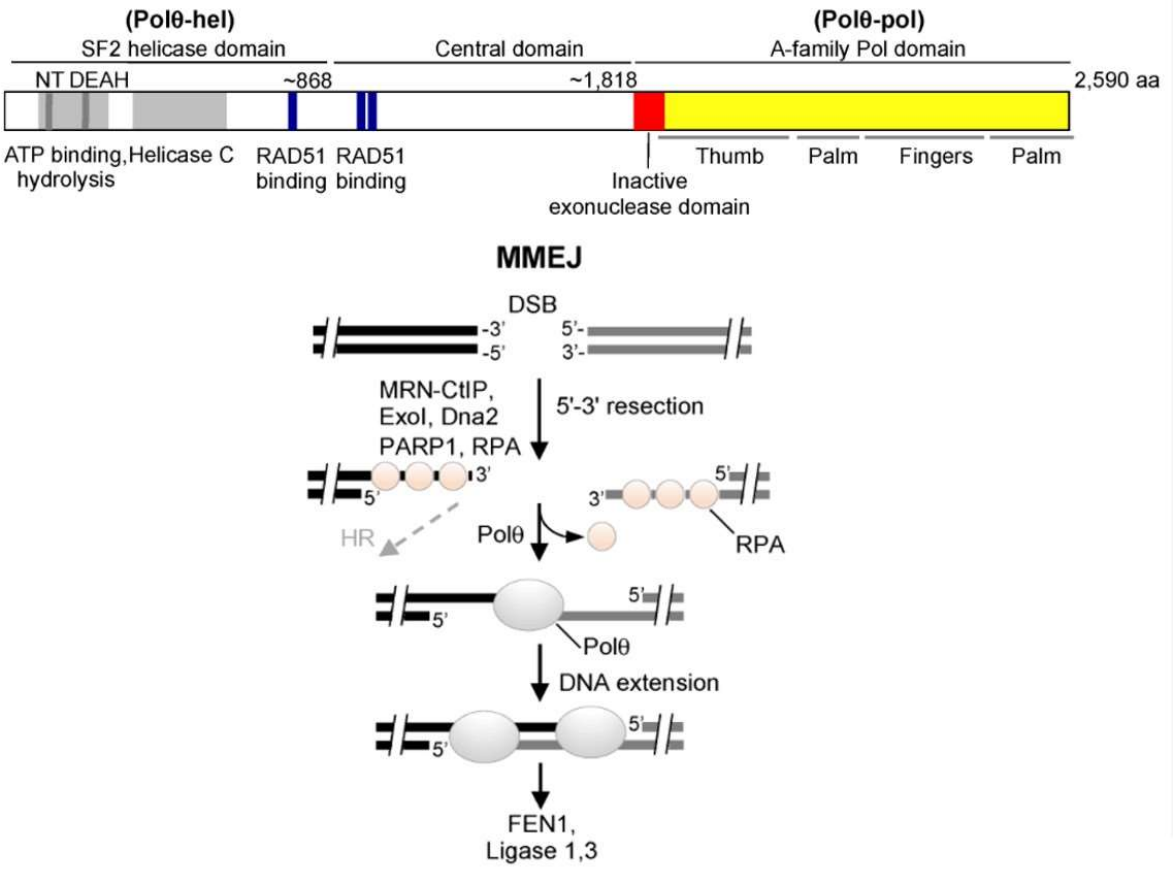

Figure 1.7.1 A schematic diagram summarising both the structure of POLQ and the role it undertakes in the DNA extension required to repair a DSB by MMEJ. This figure is adapted from Chen et al. (2021)

POLQ is an essential helicase that mediates MMEJ repair of DSB. The mechanism by which POLQ acts in MMEJ is mainly exerted through the helicase and polymerase domains, with little known about the function of the central domain. The POLQ-hel domain is thought to promote annealing in short tracts of complimentary ssDNA (60) .Furthermore, POLQ-hel contains Rad51 binding motifs, which prevent the protein from performing the homology search that underpins HR (61). The POLQ-pol domain is associated with the error-prone synthesis of DNA used in MMEJ and TLS (60). It is understood that, like HR, MMEJ initiation requires 5'-3' resection of the DSB performed by

short-range resection factors. The resection is limited and serves to reveal small microhomologies, which are substrates for POLQ-mediated end joining (62). Typically,

MMEJ is very error-prone and often results in base deletions ranging between 50-300bp (63). POLQ deficiency was demonstrated to be synthetically lethal with HR deficiency, usually in BRCA1/2 mutated models. Higgins *et al.* demonstrated that siRNA depletion of POLQ was capable of radiosensitising various pre-clinical tumour models irrespective of BRCA mutation status and, therefore, posited the idea of POLQ inhibitor-mediated radiosensitivity using small-molecule inhibitors (64).

1.8 DNA polymerase theta inhibitors as radiosensitising agents

Many large discovery programs have been put in place to target POLQ using inhibitors, even before its role in MMEJ was characterised. The main aim of these programmes was to exploit the synthetic lethality between POLQ and HR that many had observed (45,61,65). The synthetic lethality of POLQ and HR has been shown to stem from POLQ's anti-recombinase activity (45,61). The seminal work of Mateos-Gomez et al. involved the depletion of Lig4 and Shelterin in mouse embryonic fibroblasts (MEF) to promote more resection-based repair mechanisms like HR and MMEJ. A chromosome-orientation fluorescence *in situ* hybridisation (CO-FISH) assay was performed to assess the exchange of telomeres between sister chromatids (a marker of HR) as well as telomere fusion (a marker of MMEJ). Whilst a depletion of POLQ caused an expected decrease in levels of telomere fusion, the depleted POLQ also caused an increase in telomere exchange between the sister chromatids (45). To further verify this, I-Sce1 was used to generate a DSB in Lig4-depleted MEFs and flow cytometry was used to quantify the levels of each repair mechanism used. When POLQ was depleted, and an I-Sce1-induced DSB was introduced, HR was the predominant mechanism of repair. This posited the theory of POLQ-mediated MMEJ acting as a backup repair mechanism when HR was impaired. This was verified in co-depleted POLQ and BRCA1/2 MEFs which displayed

significantly increased amounts of chromosomal instability (45). Separate work conducted by Ceccaldi et al. in the same year concluded that the depletion of POLQ activity demonstrated an increased level of HR repair in epithelial ovarian cancer models (61). The results of this seminal work highlighted the POLQ/HR synthetic lethality and paved the way for the development of POLQ inhibitors as antitumour agents.

Following an extensive high-throughput screen, Zatreanu *et al.* sought to identify inhibitors of the POLQ gene that had IC_{50} values within the lower micromolar range. From this work, the compound ART558 was discovered. It is important to note that ART558 inhibits the polymerase domain of POLQ, unlike novobiocin, which targets the helicase domain. The compound allosterically binds to and inhibits POLQ at its polymerase catalytic domain (66). The screen also revealed another POLQi, ART615 however, this compound couldn't inhibit more than 10% of POLQ's activity even at concentrations of 12μM, so this was left as a control for ART558 as the two compounds are isomers(67). ART558 uniquely inhibits POLQ, and using a nanoluciferase-encoding TMEJ reporter substrate, Zatreanu et al. were able to show ART558 dose-dependently reduces the amount of MMEJ occurring, whilst ART615 had no effect. ART558 was also shown to be synthetically lethal with BRCA1/2 and 53BP1 *in vitro*. ART558 is not well tolerated *in vivo* due to poor metabolic stability therefore, ART899 was developed soon after. ART899 elicited similar *in vitro* results when tested by the luciferase-based reporter system to quantify the amount of MMEJ occurring in HEK293 cells. ART899 had an IC_{50} of 180 nM compared to ART558's 150 nM (68). This compound was, therefore, used in future *in vivo* work due to its increased metabolic stability. Whilst Zatreanu's work showed a synthetic lethality between HR-deficient tumour models and POLQ inhibition, Rodriguez et al. demonstrated that ART558 also can radiosensitise HR-proficient tumours at concentrations as low as 1 μmol/L. The means by which POLQi mediate radiosensitisation was also alluded to as treatment with POLQi and IR, which led to an increase in 53BP1 and gH2AX foci,

indicating the radiosensitisation mechanism is based on DDR impairment (68). The mechanism by which 53BP1 works is thought to be through an effector molecule known as the Shieldin complex, a known antagonist of resection (52). SHLD2 is the most commonly mutated subunit of the whole complex, with prostate cancer having a large proportion of SHLD2 deletions. Each subunit in the Shieldin complex is epistatic with one another as well as 53BP1. Therefore, by studying the effects of short-range resection factors (namely MRE11 and CtIP) that are believed to initiate DNA end resection using SHLD2-disrupted *in vitro* models, we may uncover exactly how SHLD2 disruption causes POLQi-mediated radiosensitisation and, the mechanism behind 53BP1 and POLQi's synthetic lethality.

Novobiocin is an example of a repurposed drug developed for radiosensitisation, originally, the antibiotic was used to treat infections by gram-positive bacteria. DNA gyrase is a type II topoisomerase found exclusively in bacteria that introduces negative supercoils into bacterial DNA, novobiocin binds to this complex and inhibits it, eliciting antibacterial effects (69). Zhou et al. were the first group to present novobiocin as a POLQi following a small molecule screen (70). Novobiocin acts by binding to the helicase domain of the POLQ protein, thus inhibiting any ATPase activity the polymerase may have, limiting its ability to facilitate MMEJ. In HR deficient tumour models, particularly those with BRCA1 mutations, MMEJ is heavily relied on, and often, these tumours have high expression of POLQ. Therefore, in HR-deficient models, treatment with novobiocin results in excess end resection and accumulation of DNA damage, which leads to cell killing (70). Novobiocin is currently recruiting for a phase I clinical trial evaluating its safety as an anticancer agent in tumours deficient for DDR genes (NCT05687110).

1.9 Outline and purpose of the thesis

The largest impediments to RT as a treatment option remains the presence of radioresistance. As such, we must continue to evaluate novel compounds for their ability to radiosensitise cancer cell populations to improve the efficacy of RT in the clinic. The work presented in this thesis will summarise an MRes project split into two halves, separately evaluating two potential radiosensitising agents: MangaCisTEX and ART558.

Aim of Project I

The MangaCisTEX work hypothesised that the drug would radiosensitise lung cancer models. This was tested *in vitro* using a resazurin-based viability assay on A549 and H1299 cell lines. The results show that MangaCisTEX fails to radiosensitise lung cancer cell models *in vitro*. Additionally, cisplatin (IV) was shown to display single-agent toxicity as a prodrug, calling into question the purported non-toxicity of platinum (IV) compounds. Finally, insight was provided into the effects of the novel Texaphyrin MMn when used as a single agent.

Aim of Project II

The investigation into ART558 as a POLQi hypothesised that DNA end-resection was the driver of POLQi-mediated radiosensitivity in SHLD2-disrupted cells. This was tested using an *in vitro* prostate cancer model, 22RV1, as this is where shieldin mutations are most prevalent. Using 40 nM siRNA, we were able to deplete short-range resection factors and observe the effect of ART558 on WT and SHLD2 KO cells by clonogenic survival assays. The results suggest that at low concentrations of inhibitor, CtIP is involved in POLQimediated radiosensitisation but becomes less so when the concentration of the inhibitor is increased. The data also seems to suggest that POLQi-mediated radiosensitisation does not involve MRE11.

Chapter 2: Materials and Methods

2.1 Tissue Culture

A549 (human lung adenocarcinoma) and H1299 (human large cell lung carcinoma) were purchased from the American Type Culture Collection (ATCC), they were selected for their translational relevance in testing the cisplatin alternatives as cisplatin (II) is used when treating locally advanced NSCLC patients with chemoradiotherapy. A549 and H1299 were maintained in Dulbecco's modified Eagle medium (DMEM, Sigma-Aldrich) and RPMI-1640 (RPMI, Sigma-Aldrich), respectively.

22RV1 WT (prostate) and 22RV1 SHLD2 KO were kindly given to us by our collaborators, Artios Pharma. This cell line was selected as SHLD2 is mutated in 6-13% of prostate cancers, making 22RV1 a translationally relevant model and a suitable parental line from which a SHLD2 KO could be generated. Furthermore, this cell line forms colonies, making them suitable for use in colony formation assays. Both the WT and KO cells were maintained in RPMI (Sigma-Aldrich).

All media utilised in Project I and Project II were supplemented with 10% foetal bovine serum (FBS, Gibco) and 1% Penicillin-Streptomycin (PenStrep, Sigma-Aldrich). All FBS aliquots used were from the same serum batch. Upon receipt, cells were expanded and frozen down for liquid nitrogen storage. When in culture, cells were stored at 37ºC and 5% CO_2, regularly being passaged at approximately 80% confluency. Flasks were then discarded after being in culture for 4-6 weeks. All cell lines were authenticated by LCG standards (ATCC) using short tandem repeat (STR) profiling. This is a procedure where STR on the DNA are extracted, amplified and separated by electrophoresis. The STR locus fragment size will be proportional to the number of repeats, and this can be compared with reference databases to confirm the identity of the cell line. These were carried out biannually. Prior to freezing down and after thawing cell stock, small amounts

of supernatant were used to test for the presence of mycoplasma using the MycoAlert testing kit (Lonza).

2.2 Irradiation

All irradiations were carried out using a GSR D1 Caesium-137 irradiator with a maximum activity of 200TBq (Gamma-service Medical, GMBH). As a result, all experiments conducted both in Project I and Project II were conducted using the gamma radiation provided by the irradiator at a dose rate of 1.1 Gy/min.

Methods I: MangaCisTEX

2.3 Drugs and Solubility Testing

MangaCisTEX, MMn, MGd and cisplatin (IV) were gifted to us by Adam Sedgwick from King's College London (formerly of Texas University, Austin) in their powdered form. Cisplatin (II) (Merck) was purchased commercially in powdered form also. We utilised alamarBlue™ cell viability assays to test these drugs *in vitro* at varying concentrations. The first step was a series of solubility tests to determine the correct diluent for drug reconstitution.

DMSO is a very widely used solvent and is usually the first option when looking to dissolve a drug in powdered form. However, the work of Hall *et al.* has shown that the nucleophilic sulphur of DMSO complexes with platinum alters the structure of the agent, affecting its ability to initiate cell death (71). Therefore, alternative solvents were investigated. For cisplatin (IV) and (II), it seemed that using sterile water sufficed for the full solvation of the drug. However, this was not the case for MMn or MangaCisTEX, both of which were highly insoluble. It was decided that dissolving these two drugs was improbable without the use of DMSO. Therefore, each drug was diluted with 1% DMSO and 99% sterile water. This ensured that when used in experiments, the overall

concentration of DMSO in the well would be 0.002% v/v, which is negligible and shouldn't affect the cytotoxicity of the platinum agent. Using this combination of solvents was successful and resolved the issue of the insoluble drug powders. MGd was dissolved in 5% dextrose as advised by our collaborator. The table below summarises the reconstitution of each powdered drug to make a stock solution (Figure 2.3.1)

Drug	Solvent	Concentration of stock solution
MMn	1% DMSO + Water	10mM
MangaCisTEX	1% DMSO + Water	10mM
MGd	5% Dextrose	10mM
Cisplatin (IV)	Water	6mM
Cisplatin (II)	Water	6mM

Figure 2.3.1 Table summarising the reconstitution of all drug powders into their stock solutions for use in the cell viability assay. "Water" refers to sterile water.

2.4 Cell viability assays

alamarBlue™ cell viability assays were used to assess the radiosensitising effects of MangaCisTEX, MMn, cisplatin (IV), cisplatin (II), MGd, MGd+ cisplatin (IV) and MMn+ cisplatin (IV). For each of the seven drug conditions, there was an unirradiated arm and an irradiated arm (single radiation fraction of 4 Gy). The radiosensitising effect of these drugs was studied in two lung cancer models, A549 and H1299.

On day 0, cells were harvested from a stock culture of approximately 80% confluency and counted on a LUNA-II™ Automated Cell counter (Logos Biosystems). Both A549 and H1299 cells were seeded at densities of 175 cells/well for the unirradiated condition and 400 cells/well for the irradiated condition, both in 175 µL of cell suspension. Cells were seeded into flat-bottom, 96-Well TC-treated microplates (Corning) in their respective media (DMEM or RPMI) supplemented with 10% FBS and 1% PenStrep. TC-treated

plates were selected as they facilitate the optimum growth and attachment conditions for anchorage-dependent cells such as the cell types we used. The seeded cells were left to incubate at 37ºC and 5% CO_2 for four hours to allow for cell adherence.

During the incubation period, the drugs were reconstituted from their powdered forms using the aforementioned solvents (highlighted in Figure 2.3.1). These stock solutions were then further diluted in the appropriate media. In order to obtain the desired drug concentration range in the well, 25µL of the drug suspension was added to each well to achieve a final concentration of 0.66, 1.25, 2.5, 3.75, 5, 7.5, 10, 15 and 20µM for each drug condition at a total 200µL of suspension. DMSO-treated cells were seeded as a positive control, and wells with 100µL media and no cells (blank) were kept as experimental controls. Finally, PBS was added to all other wells to mitigate the edge effect where evaporation could cause variability in fluorescence readouts (see Figure 2.4.1).

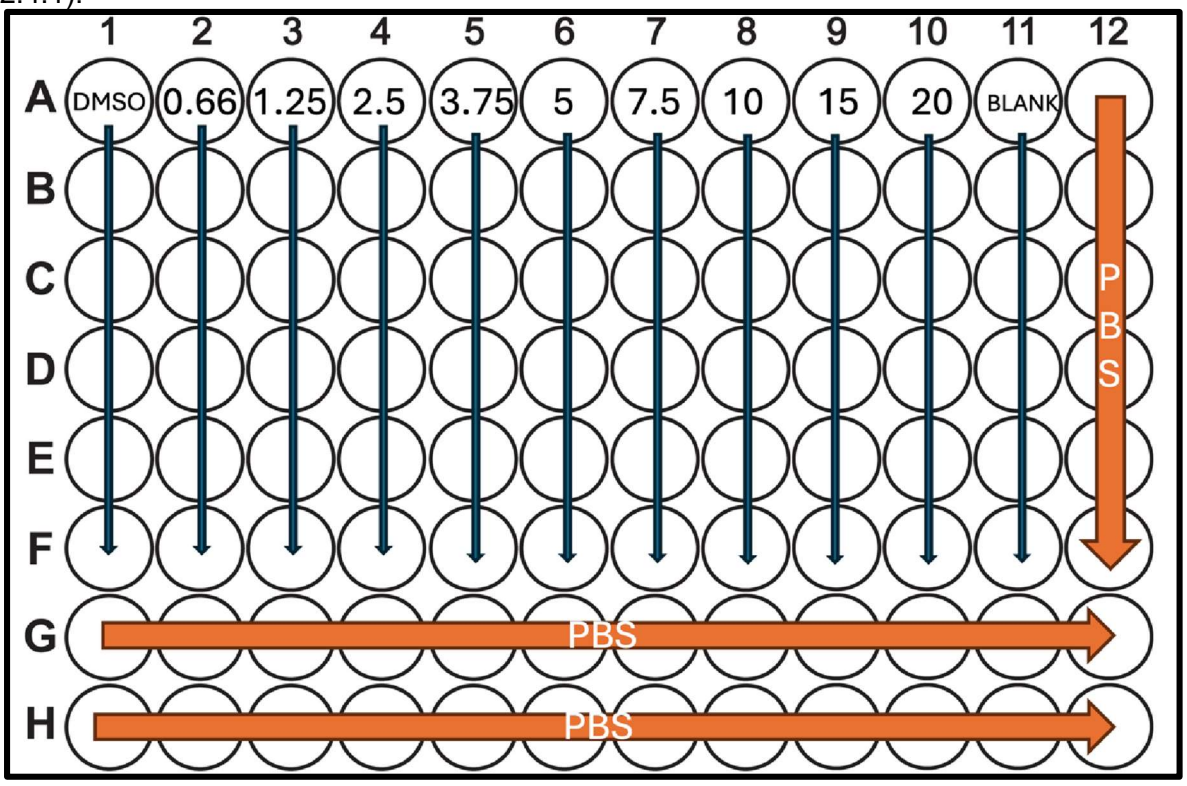

Figure 2.4.1 Diagram depicting the layout of the 96-well plate used for the cell viability assay with 9 total concentrations tested per drug. There was also a lane of DMSO-treated cells to act as the positive control and a lane of "blank" non-cell-containing media to act as an experimental control. PBS was added to all other wells.

As cisplatin (II) is light-sensitive, all other drugs tested were treated as such and kept protected from light, the treatment of each plate was done under safety cabinets with the lights switched off. Drug administration occurred four hours post-seeding, and the drug was left in the plate for two hours to allow enough time for adequate cellular uptake of the drug. Two hours after drug administration, the plates from the irradiated arm were exposed to a single fraction of 4 Gy IR (details in section 2.2). Once returned to the incubator, all plates were then left to incubate for eighteen hours overnight (the average doubling time for each of these cells), meaning the cells had a total drug interaction time of twenty hours (workflow illustrated in Figure 2.4.2). On day 1, the media containing the drug was discarded and replaced with 100µL of either DMEM (A549) or RPMI (H1299). The experimental blank was left to not transfer any cells into the well when using the multichannel aspirator. After discarding the drug and replacing the media, the plates were then left for cells to proliferate until the DMSO-treated well reached 70-80% confluency, indicating the plate was ready for staining with alamarBlue™ reagent.

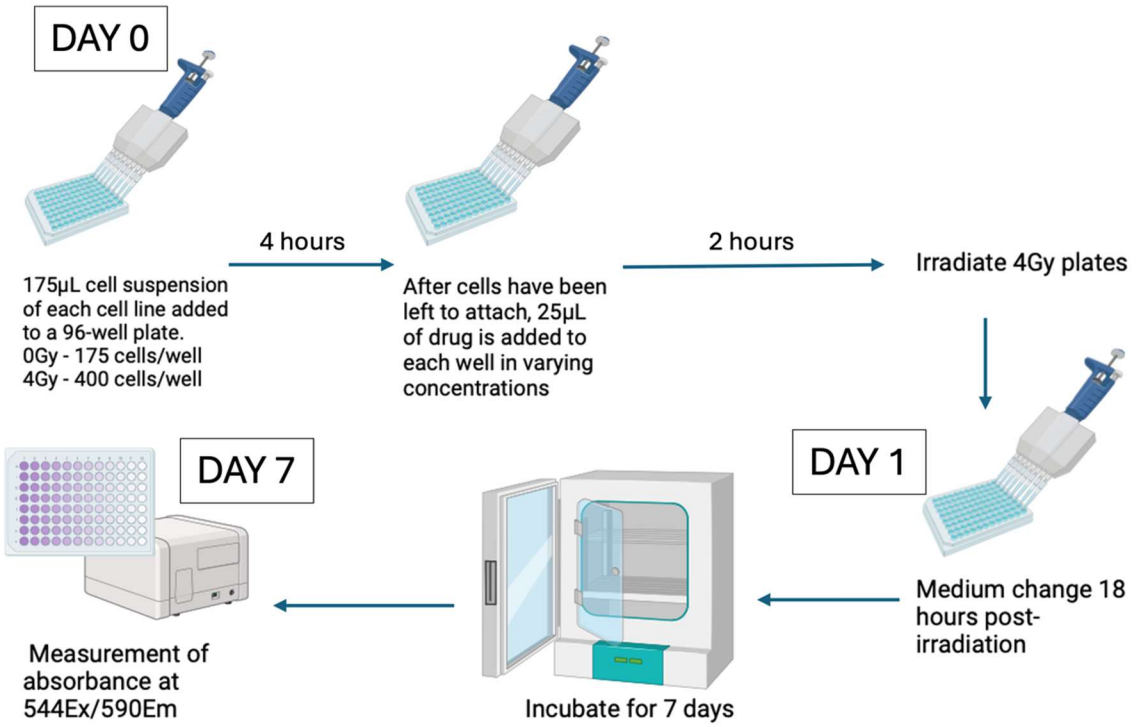

Drug(s) tested	MangaCisTEX
	MMn
	MMn+ cisplatin (IV) – separate agents unconjugated
	MGd+ cisplatin (IV)
	Cisplatin (IV)
	Cisplatin (II)
	MGd

Figure 2.4.2 Schematic diagram illustrating the overall steps in the methodology of an alamarBlue™ as well as a table illustrating the different drug(s) that were tested. Created in Biorender.com.

alamarBlue™ is a resazurin-based dye often used to quantitatively measure cell viability *in vitro*. Metabolically active cells possess lactate dehydrogenase that will catalyse the reduction of resazurin (blue) to resorufin (red), and this reaction emits fluorescence at 590 nm. alamarBlue™ dye was prepared from a powder (Sigma-Aldrich) at a working concentration of 1 µg/mL diluted in sterile PBS. The diluted resazurin dye solution was then sterile-filtered using a polyethersulfone (PES) membrane filter unit (Merck). The

sterile resazurin dye was aliquoted and stored at -20ºC. The plates reached the desired confluency on day seven and were stained with the prepared aliquots of alamarBlue™.

Due to the viscous nature of the resazurin dye, we found it necessary to further dilute the 1 µg/mL stock in culture media to achieve a final concentration of 0.2 µg/mL, i.e. one-part alamarBlue™ aliquot diluted in four-parts culture media making a new working solution. 100 µL of the new working solution was added to each well, giving a total well volume of 200 µL, and the plates were left to incubate at 37ºC for three hours. Following the incubation, a fluorescent readout was obtained by a POLARstar Omega microplate reader (BMG Labtech) at 544/590 nm excitation/emission.

There were six replicate wells per drug concentration in the cell viability experiments, for which the mean fluorescence and standard deviation (SD) were calculated. The mean fluorescence of the blank wells was subtracted from that of each drug concentration, and each concentration was normalised to the mean DMSO-treated fluorescence (setting DMSO-treated cells to 100%). This can be summarised by the following formula:

$$Normalised\ Fluorescence = \frac{(Mean\ fluorescence_{!"\#\$} - Mean\ fluorescence_{\%\&'()}) \times 100}{Mean\ fluorescence_{*+,-}}$$

Due to the coefficient of variation, SD was normalised by accounting for differences in the mean and can be summarised by the following formula:

$$Normalised\ SD = \frac{(SD_{!"\#\$})}{Mean\ fluorescence_{*+,-}} \times 100$$

The calculation of both the normalised fluorescence and normalised SD for each drug concentration was used in subsequent statistical analysis (detailed in section 2.7).

Methods II: POLQi

2.5 siRNA Transfection and Clonogenic Survival Assays

Clonogenic survival assays are considered the gold standard when it comes to the *in vitro* assessment of radiosensitising agents. We utilised this assay to observe the extent to which two different POLQi concentrations radiosensitise 22RV1 WT and SHLD2 KO cell lines and how depletion of short-range resection factors can reverse or "rescue" radiosensitivity.

To investigate the role of resection in POLQi-mediated radiosensitivity, a series of rescue experiments were performed by clonogenic survival assay using 40nM siRNA (details in figure 2.5.1) to silence short-range resection factors (MRE11 and CtIP/RBBP8) in 22RV1 WT and SHLD2KO. We used siMRE11 (cat#4390824, ThermoFisher), siCtIP (cat# 4392420, ThermoFisher) from the Silencer™ Select siRNA library and siNT (non-targeting control) (cat#4390844, ThermoFisher).

Target gene	Sense sequence (5' -> 3')	Concentration	Company
MRE11	GAUAGACAUUAGUCCGGUUtt	40 nM	ThermoFisher
CtIP	GUACAAGGUUUACAAGUAAtt		
NT	No sequence provided		

Figure 2.5.1 A table that summarises the details of siRNA used to deplete short-range resection factors as well as the non-targeting control used.

On day 0, cells were harvested from 80% stock culture and counted on a LUNA-II™ Automated Cell counter (Logos Biosystems). Cells were seeded for three experimental conditions in each cell line: siNT (non-targeting control), siMRE11 and siCtIP. 125,000 cells/well were seeded for 22RV1 WT and 250,000 cells/well for 22RV1 SHLD2 KO in 2 mL cell suspension. Each siRNA was diluted in serum-free media, OptiMEM (Gibco) and incubated with Lipofectamine™ RNAiMax transfection reagent in a 1:1 ratio for twenty minutes at room temperature (RT). 500 µL of this transfection complex was added to the cell suspension before cell adherence began, and plates were incubated at 37ºC for 72

hours to allow for silencing of short-range resection factors. All knockdowns were verified by immunoblot.

On day 3, transfected cells were harvested from 80% confluent transfection plates and counted on a LUNA-II™ Automated Cell counter (Logos Biosystems). Cells were seeded at the following densities (Figure 2.5.2).

Radiation dose	22RV1 WT (cells/well)	22RV1 SHLD2 KO (cells/well)
0Gy	1600	1600
3Gy	3200	16,000

Figure 2.5.2 – A table illustrating the seeding densities in 2 mL cell suspension used when performing the clonogenic survival assay.

The transfected WT and KO cells were seeded into flat-bottom, 6-Well TC-treated plates (Corning) in RPMI supplemented with 10% FBS and 1% PenStrep. ART558 was kindly gifted to us by collaborators at Artios Pharma, and this arrived in powdered form before being reconstituted in DMSO to make a 12mM stock solution. The stock solution of ART558 was then further diluted in RPMI to achieve the desired final concentration. Following the work of Rodriguez-Berriguete *et al.*, the concentration of ART558 was seen to exhibit radiosensitising effects at 1 μM, with 3 μM demonstrating a radiosensitisation that was greater than or equal to that of the 1 μM treatment group (68). Therefore, we selected to treat the transfected cells with either 2 μM DMSO/ART558 or 4 μM DMSO/ART558 four hours post-seeding. Each drug condition was assessed in triplicate (illustrated in Figure 2.5.3). The plates were incubated following drug administration for 1 hour before either being left unirradiated or receiving a single fraction of 3Gy IR (details in section 2.2). All plates were then incubated at 37ºC for 72 hours before the drugcontaining media was discarded and replaced with 2000μL of fresh RPMI. The plates were left to incubate and form colonies before being stained by crystal violet approximately three weeks later. Crystal violet fixes the plates and stains colonies a deep purple that allows us to visualise and count colonies using GelCount™ (Oxford Optronix).

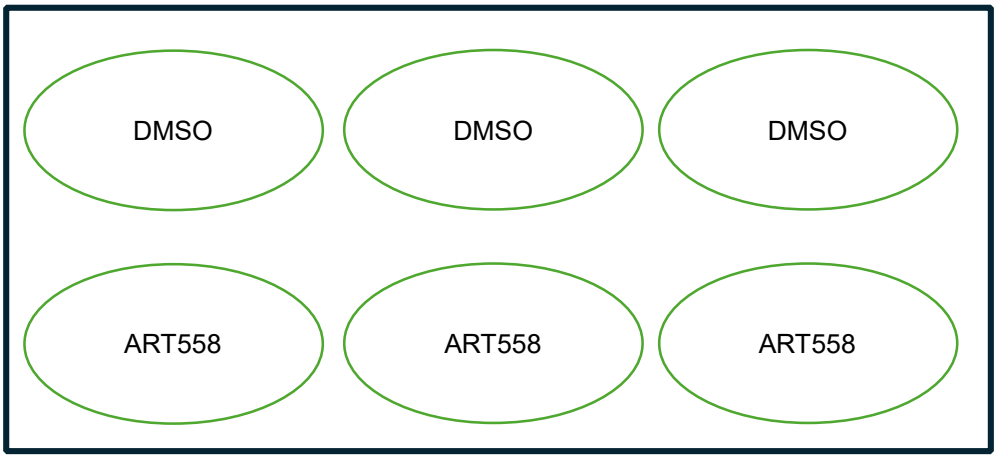

Figure 2.5.3 Image describing the plate setup for the seeding of clonogenic. For the 2 μM and 4 μM experimental arms, DMSO and POLQi were seeded in triplicate. Each plate was seeded using WT or SHLD2 KO cells with either siNT, siMRE11 or siCtIP transfections.

Colony counts obtained from the GelCount™ were used to calculate plating efficiency with the following formula:

$$Plating\ \ efficiency\ \ (PE)\ \ (\%) = \frac{No.\ of\ \ colonies}{Cells\ \ seeded} \times 100$$

Surviving fractions (SF) were calculated by the following formula:

$$Surviving\ \ fraction_{./0} = \frac{PE_{./0}}{PE_{1/0}}$$

As a result, all SF for the unirradiated condition were 100%, and the SF for the irradiated condition were used to calculate the radiopotentiation factor (RPF) with the following formula:

$$RPF = \frac{SF_{*+,-}}{SF_{234556}}$$

2.6 Immunoblotting

All siRNA knockdowns were confirmed by immunoblot. Following the three-day transfection period and cell seeding for the clonogenic survival assay, the transfected cells left over were returned to the 6-well plate. This transfection plate was incubated at 37ºC with the experimental plates for 5 hours until the point of experimental irradiation.
When the experimental plates were irradiated, the transfection plate was washed with PBS and then frozen down to ensure the immunoblot result would show the extent of gene knockdown at the time the experiment was performed.
To perform the immunoblot, the first step was to isolate the cell lysate from the frozen transfection plate.

The working lysis buffer solution was made up of 1 mL radioimmunoprecipitation assay buffer (RIPA) (Cat#89900, ThermoFisher), 143 µL 7x protease inhibitor cocktail (Cat#11836153001, Roche) and 10 µL phosphatase inhibitor cocktail (Cat#P5725, Sigma). The working lysis buffer was kept on ice. Once the transfection plates had thawed out, a small volume of this lysis buffer solution was added. The volume of buffer solution added was calculated by halving the percentage confluency prior to freezing down. The cells were then scraped, and the lysate was transferred to an Eppendorf tube for sonication using a Digital Sonifier® (Branson) at 10% amplitude for 10 seconds. The Eppendorf was centrifuged at 4ºC and 25,000 RPM (Heraeus Pico Biofuge) for 10 minutes to ensure all cellular debris would collect as a pellet at the bottom. Finally, the supernatant was transferred to a new Eppendorf tube, giving the protein lysate that would be used for the immunoblot.

To determine protein concentration in samples and allow for equal protein loading, a Bicinchonic assay (BCA) was performed using the Pierce™ BCA protein assay kit (Cat#23225, ThermoFisher). A set of protein standards was made up using varying

volumes of 2 µg/mL BSA from the kit and distilled water (dH_2O). In the BCA protein assay kit, there is Reagent A, which contains BCA amongst an alkaline solution of sodium bicarbonate, sodium carbonate, sodium tartrate and sodium hydroxide. There is also reagent B, which contains copper (II) sulphate pentahydrate, providing the Cu^{2+} ions that are reduced to Cu^{+} in the presence of protein (biuret reaction). Reagents A and B were mixed at a ratio of 49:1 and combined with known concentrations of BSA to form a standard curve. Reagents A, B and dH_2O were mixed at a ratio of 47:1:2 and combined with 2 µL of protein lysate to form the sample, and this was left to incubate at 37ºC for 30 minutes. Following the incubation, an absorbance readout was taken with a POLARstar Omega microplate reader (BMG Labtech). The absorbance readout of the samples was normalised to those of the BSA standards, and the protein content of the sample was determined.

The final solution needed for the immunoblot was the loading buffer, comprising 200 µL of LDS loading buffer (Cat#NP0007, ThermoFisher) and 10 µL of 1M Dithiothreitol (DTT) (Cat# M109, VWR). All samples were an equal volume of 35 µL comprising protein lysate, 8.75 µL of the loading buffer+DTT and the remaining volume was made up by RIPA buffer. When mixed, the Eppendorf was heated at 95ºC for 5 minutes before being centrifuged for 1 minute. Samples were loaded into the wells of 4-20% Mini-PROTEAN TGX precast 10-well protein gels (Cat#4561094, Bio-Rad) and ran at 80 V for 30 minutes and then 120 V for a further hour.

The gel was removed from the cassette and placed on a trans-blot nitrocellulose pack (Bio-Rad). Using the trans-blot turbo transfer system (Bio-Rad), the protein was transferred to a nitrocellulose membrane, successful transfer was confirmed by Ponceau S, Acid Red (Cat# P7170, Sigma-Aldrich). The membrane was blocked for an hour with either 5% milk-TBST (MRE11) or 2% BSA-TBST (CtIP), ensuring the blocking solution was the same as the primary antibody diluent. During the 1 hour blocking time, the

primary antibodies were prepared (shown in Table 2.5.1). The primary antibody was added for overnight incubation at 4ºC.

Antibody	Species	Manufacturer	Dilution	Diluent	Primary/Secondary	Cat No.
Anti-MRE11	Rabbit	Abcam	1:500	5% Milk	Primary	Ab109623
Anti-CtIP	Mouse	Active-Motif	1:500	2% BSA	Primary	61141
Anti-Rabbit	Goat	Cell signalling	1:10000	5% Milk	Secondary	7074
Anti-Mouse	Horse	Cell signalling	1:50000	5% Milk	Secondary	7076

Table 2.6.1 Summary of all antibodies used in the immunoblot protocol.

The next day, the primary antibody was recovered, and each of the blots was washed thrice with TBST before incubation with the appropriate secondary for 1 hour at RT. Following this, the blots were once again washed thrice with TBST. In order to visualise the protein on the immunoblot, we used the ECL prime detection reagent (Cat#RPN2232, Cytiva), which detects proteins on the membrane through an enhanced chemiluminescence reaction. The reagent is made up of equal parts solution A and B. Solution A contains luminol, and Solution B contains peroxide. In the presence of horseradish peroxidase (HRP, which is conjugated to the secondary antibodies), HRP will catalyse peroxide's oxidation of luminol, which emits the chemiluminescent signal. The reagent is applied to the blot and left to incubate for 5 minutes before the excess is drained, and the blot can be imaged on a ChemiDoc MP Imaging system (Bio-Rad).

2.7 Statistical Analyses

Project I

Data were analysed using GraphPad Prism software (version 10.1.0 for MacOS, GraphPad software).

First, a Shapiro-Wilk test was performed to test normality. The fluorescence data from the cell viability assays performed in all seven drug conditions failed this test and was found to be non-parametric. Therefore, a data log transformation was performed to ensure the parametric analysis could be used. Following this, a two-way ANOVA was then performed with an ad-hoc Tukey's or Šidák analysis to correct for multiple comparisons. Curve fitting was done using Prism with log(inhibitor) vs responses – variable slope (four parameters). Data are means±SD.

Project II

Data were also analysed using GraphPad Prism software (version 10.1.0 for MacOS, the GraphPad software). The RPF was input on GraphPad. A Shapiro-Wilk test was first performed to ensure data normality, which warranted the use of parametrical analysis. A two-way ANOVA with multiple comparisons was used to calculate the significance between WT and SHLD2 KO clones, and this was corrected by Tukey's post-hoc analysis. Data are means±SD.

Chapter 3: Results

As previously mentioned, this thesis summarises the work of an MRes project that separately evaluated two radiosensitising agents, MangaCisTEX (project I) and ART558 (project II). As such, the results will be separated under those subheadings.

Project I: MMn is a redox cycler analogous to MGd, thought to accumulate in tumour cells and exert its radiosensitising effects by inducing oxidative stress. The prodrug cisplatin (IV) is thought to be a physiologically inactive drug that adopts a more stable octahedral conformation, which can only exert its cytotoxic effects when reduced to cisplatin (II) by a reducing agent such as MMn. Therefore, when the two are conjugated to form MangaCisTEX, we hypothesised that it would act as a radiosensitiser of *in vitro* lung cancer models.

Project II: SHLD2 has been identified as a commonly deleted gene in prostate cancer. We have also previously observed that cells with a SHLD2 disruption are more sensitive to treatment with POLQi and RT. This project was built on the premise that POLQimediated radiosensitivity of SHLD2-disrupted cells may be dependent on DNA end resection. Therefore, we hypothesised that depletion of short-range resection factors would reverse or “rescue” radiosensitivity in the SHLD2-disrupted cells.

Results I: MangaCisTEX

3.1 MangaCisTEX fails to radiosensitise in H1299 and A549 cell lines

The underlying principle of this work was to identify a novel radiosensitising drug that could sensitise cells to the cytotoxic effects of radiation. The radiosensitising capacity of this drug was tested using alamarBlue™(referred to as cell viability assays in this section) in H1299 and A549 cells. The cells were incubated with increasing concentrations of MangaCisTEX for 20 hours (experimental details in section 2.4). To ensure the constituent moieties of the novel conjugate were acting as intended, the following positive controls were used (Figure 3.1.1).

Novel agent	**Positive control included**
MMn	MGd
Cisplatin (IV)	Cisplatin (II)

MangaCisTEX	Cisplatin (II)

Figure 3.1.1 Table highlighting the positive controls included with the novel agents when conducting cell viability assays. MGd is included as an established Texaphyrin, and cisplatin (II) is included as a comparative platinum agent (for cisplatin (IV)) as well as a cytotoxic chemotherapeutic agent that can be used as a radiosensitiser (for MangaCisTEX).

Both *in vitro* cell lines (H1299 and A549) demonstrated that MangaCisTEX does not enhance the radiosensitivity of cancerous cells (Figure 3.1.2). In the H1299 experimental arm, a single dose of 4Gy radiation had no additive effect on reducing cell viability compared to MangaCisTEX without radiation. This was further supported by the minimal difference in IC_{50} values between the unirradiated (0 Gy) and irradiated (4 Gy) groups (1.88 μM and 1.46 μM, respectively).

Similarly, in the A549 experimental arm, MangaCisTEX still demonstrated unexpected cell death in the unirradiated condition. The presence of radiation did not seem to augment the reduction in cell viability. The IC_{50} values for the 0 Gy and 4 Gy conditions were 4.88 μM and 8.63 μM, respectively. The increased IC_{50} values suggest that H1299 cells are more sensitive to treatment with MangaCisTEX than A549. However, these findings demonstrate that MangaCisTEX exhibits dose-dependent cytotoxicity that is independent of radiation in both *in vitro* lung cancer models.

The cisplatin (II) control included shows a similar trend to that of MangaCisTEX. In the unirradiated condition, there are vast amounts of cell death that are not augmented by the effects of radiation. Cisplatin (II), unlike MangaCisTEX, is an established chemotherapeutic agent that can exert cytotoxicity in the absence of radiation through the formation of inter/intra-strand DNA crosslinks. However, it is possible that our single fraction of radiation targeted cells in their G1 phase where nucleotide excision repair (NER) is upregulated (72,73). The upregulation of NER would reduce and increase the repair of cisplatin-induced DNA adducts and, therefore, reduce cisplatin's effectiveness as

a radiosensitiser. Further experiments involving the use of fractionated RT and an NER reporter assay would be needed to confirm this.

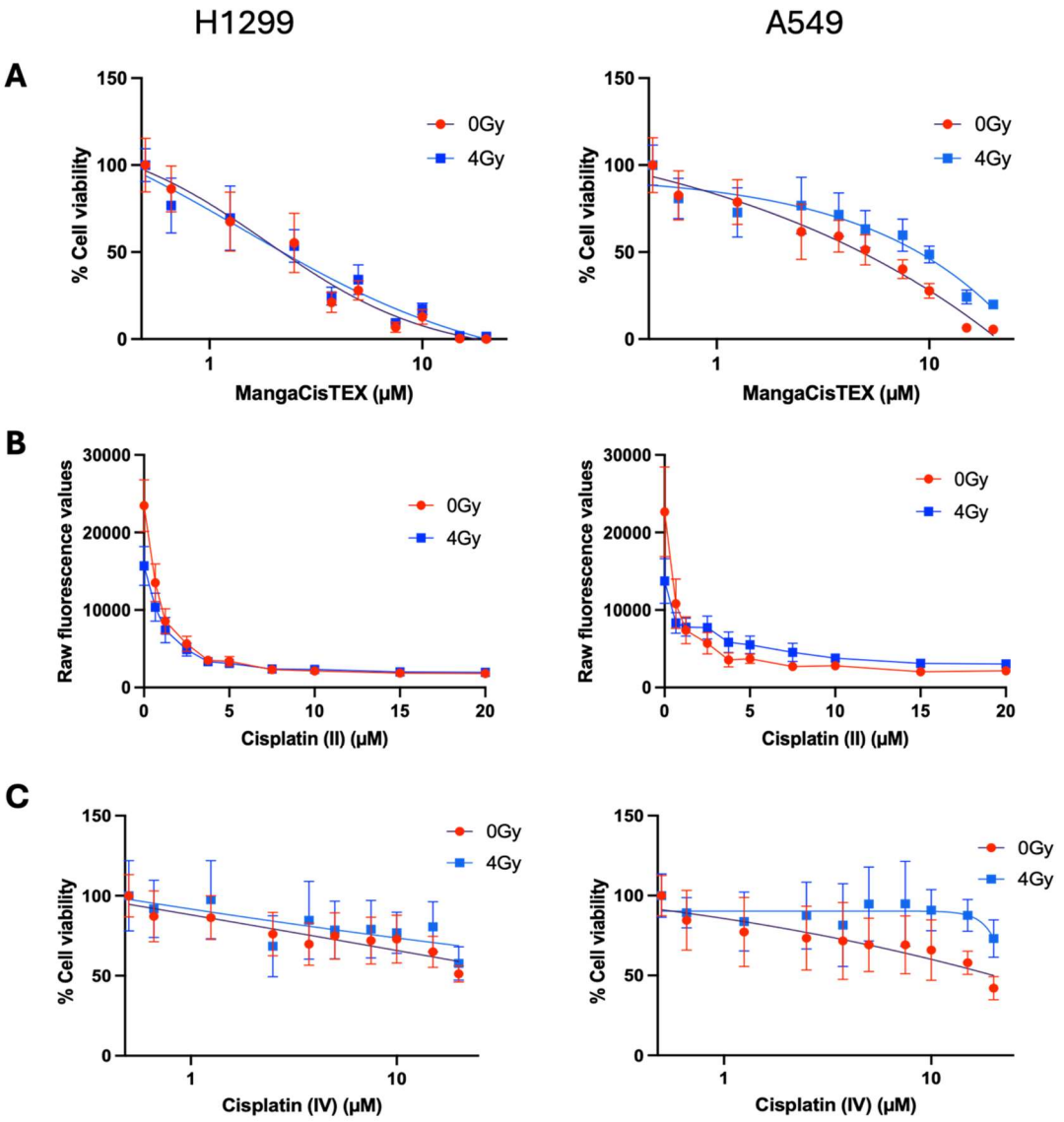

Figure 3.1.2 (A) Cell viability assay performed in two cell lines after incubation with MangaCisTEX at increasing concentrations (0-20 μM) for 20 hours. Cells remained unirradiated (0 Gy) or irradiated (4 Gy) **(B)** Same protocol as **(A)** but with increasing concentrations of cisplatin (II) as a control. (**C)** Same protocol as (**A)** but with increasing concentrations of cisplatin (IV) – a moiety in the MangaCisTEX conjugate for which cisplatin (II) was also a control.

The radiation-independent cytotoxicity of MangaCisTEX contradicted our hypotheses. Consequently, we decided to investigate the individual effects of the constituent moieties, cisplatin (IV) and MMn, to better understand their roles in the observed outcomes.

3.2 Cisplatin (IV) displays unexpected single-agent toxicity as a prodrug

Mechanistically, MangaCisTEX's radiosensitising effect is hypothesised to depend on the MMn-mediated reduction of a non-toxic cisplatin (IV) to its active, toxic form, cisplatin (II). Consequently, cisplatin (IV), when administered as a single agent, was expected to display minimal levels of toxicity when compared to cisplatin (II). 5, 10 and 20 μM of cisplatin (IV) were selected as representative concentrations to summarise the effect of low, medium and high cisplatin (IV) concentrations.

Unexpectedly, in the unirradiated H1299 and A549 cells, both 5 μM and 20 μM of cisplatin (IV) elicited significant reductions in cell viability (values summarised using the table in Figure 3.2.1). 10 μM had no differential effect when compared to 5 μM of the prodrug. When irradiated, the prodrug caused a minor augmentation of the cell killing seen in the unirradiated cells, but this was not significant, except for 20 μM of cisplatin (IV) in irradiated H1299 cells.

Cell line	Concentration of cisplatin (IV)	Radiation (Gy)	Reduction in cell viability (compared to DMSO control – 100%)	Significance of the reduction (p values)
H1299	5 μM	0	25.2%	0.0247
		4	21.4%	0.0730
	10 μM	0	27.1%	ns
		4	23.1%	ns
	20 μM	0	48.8%	<0.0001
		4	42.2%	<0.0001
A549	5 μM	0	30.9%	0.0035
		4	5.23%	0.9310
	10 μM	0	34.2%	ns
		4	9.08%	ns
	20 μM	0	58.0%	<0.0001
		4	26.9%	ns

Figure 3.2.1 A table summarising the reductions in cell viability demonstrating the varying levels of cytotoxicity caused by low, medium and high concentrations of cisplatin (IV) in H1299 and A549 cells (presented below in graphical form - figure 3.2.2).

Fundamentally, in the unirradiated condition, cisplatin (IV) should not have displayed any levels of cytotoxicity as it is an inactive prodrug requiring reduction to cisplatin (II) to exert cytotoxic effects. However, the data has shown that in unirradiated H1299 and A549 cells, cisplatin (IV) exhibits radiation-independent cytotoxicity like cisplatin (II) but just at lower levels (Figure 3.1.2).

Cisplatin (IV)'s reduction to cisplatin (II) is only facilitated by MMn in the context of MangaCisTEX, where the two moieties are conjugated, and the MMn can act as a cage for the prodrug. Cisplatin (II) was included as a control to demonstrate the action of a

cytotoxic platinum agent whilst allowing us to verify that the cisplatin (IV) prodrug is nontoxic in comparison. Whilst we expected cisplatin (IV) to remain a non-toxic prodrug when administered as a single agent, it is possible that other reducing agents in the cellular environment could cause its reduction to cisplatin (II), allowing it to exert cytotoxic effects. This is one possible explanation for the cell killing that cisplatin (IV) induces in the absence of radiation.

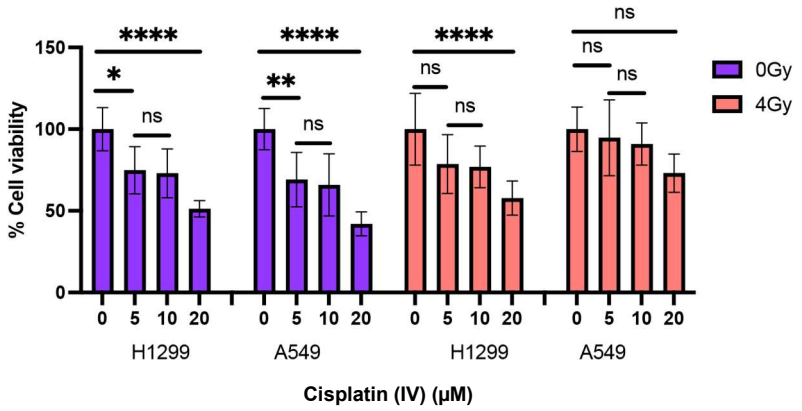

Figure 3.2.2 Bar charts illustrating the cell viability at 0, 5, 10 and 20 μM for both cell lines in the presence and absence of irradiation to assess drug cytotoxicity at low, medium and high concentrations. Analysed by 2-way ANOVA and Tukey's corrections (*, $p<0.05$, **, $p<0.01$, ****, $p<0.0001$, ns, not significant).

3.3 MMn radioprotects in H1299 and A549 cancer models

Following the investigation into cisplatin (IV)'s individual effects, we next looked at MMn. The fundamental reason for generating a manganese-based Texaphyrin was based on clinical trial data showing that MGd did not have a significant effect on survival when combined with WBRT (25). So, when testing MMn, MGd was included as a control and very similar results were expected from the two Texaphyrins *in vitro*. Mechanistically, it was thought that both compounds are redox-cycling and are expected to generate ROS species that will place the cell under oxidative stress, making it more susceptible to radiation. It was predicted that in the unirradiated condition, a minor reduction in cell viability may be visualised due to low levels of cellular oxidative stress. When irradiated, the levels of redox cycling would be amplified and, therefore, increase oxidative stress,

making the cells radiosensitive. Once again, 5, 10 and 20 μM MMn have been selected to summarise the effects of low, medium and high concentrations of MMn.

The MGd control showed a decreased amount of cell viability in the irradiated condition when compared to the unirradiated condition in both cell lines. Whilst radiation augmented MGd's cytotoxicity, this radiosensitisation was not statistically significant. This was expected as we understand MGd to not be an efficient radiosensitising agent.

In contrast, MMn displayed a surprising radioprotective effect as opposed to the radiosensitising effect we had hypothesised. The changes in H1299 cell viability are highlighted in the table below (Figure 3.3.1).

Concentration of MMn	**Cell viability$_{irradiated}$- Cell viability$_{unirradiated}$**	**Significance**
5μM	38.7%	p = 0.0005
10μM	41.4%	p=0.0002
20μM	35.5%	p=0.0016

Figure 3.3.1 A table summarising the increases in cell viability between the unirradiated and irradiated H1299 cells showing the statistically significant radioprotective effect of low, medium and high concentrations of MMn.

In the A549 model, 5 μM and 10 μM of MMn treatment seemed to display signs of possible radioprotection, with numerical increases in cell viability however, these differences were not statistically significant. Only at 20 μM MMn in irradiated A549 cells do we see a significant radioprotective effect, causing a 41.7% increase in cell viability (p=0.0001).

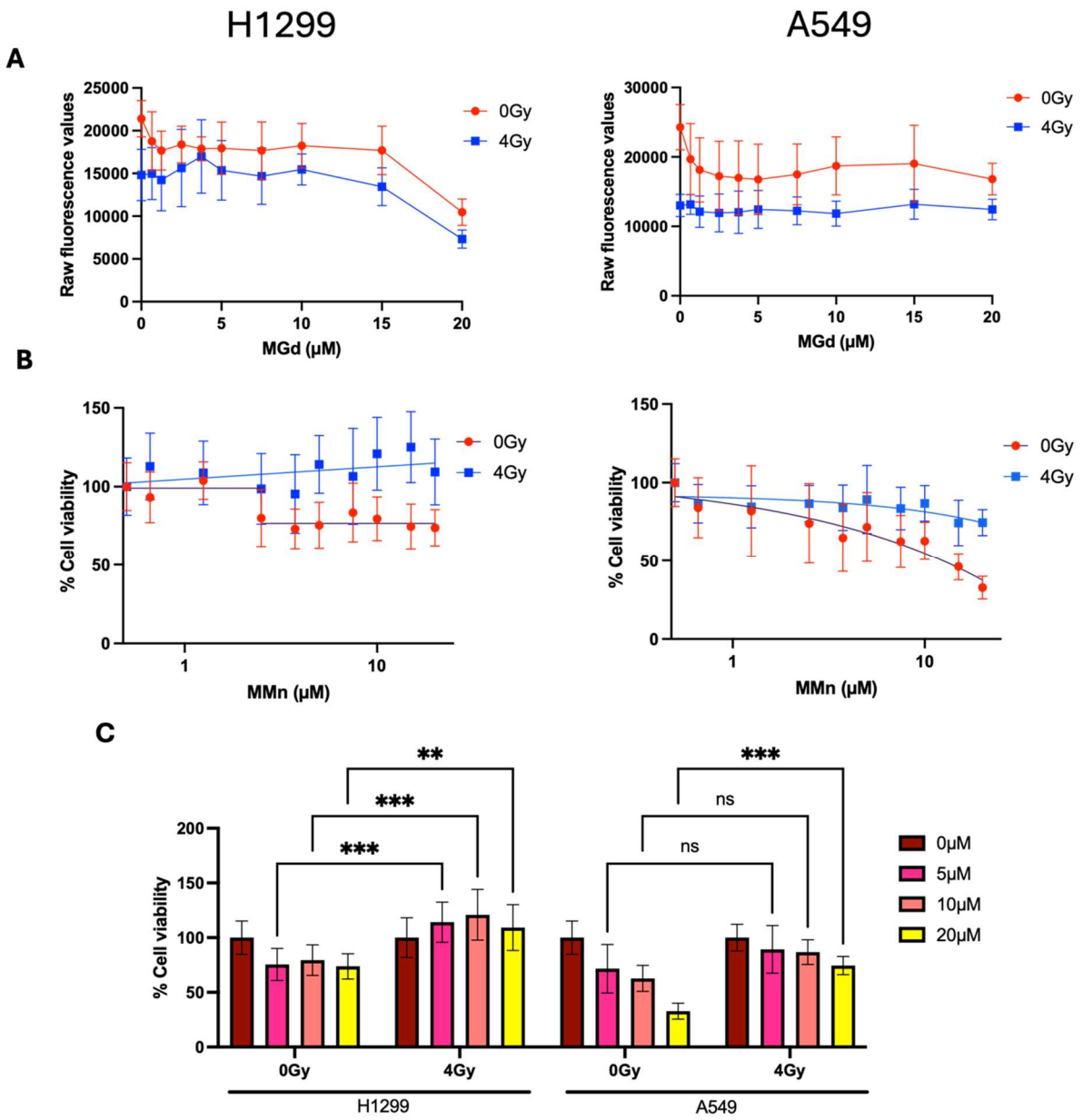

Figure 3.3.2 (A) Cell viability assays for increasing concentrations of MMn performed in both cell lines. **(B)** Same assay as (A) but with increasing concentrations of MGd. **(C)** Bar graphs comparing the cell viability of 0 Gy and 4 Gy treatment groups when each cell line is treated with 0, 5, 10 and 20μM of MMn to demonstrate radioprotection in low, medium and high concentrations of MMn. Analysed by 2-way ANOVA with ad-hoc Šidák corrections (**, p<0.01, ***, p<0.001, ns, not significant).

In the context of the hypothesis for Project I, the data presents unexpected results. Contrary to our expectations, MangaCisTEX failed to exhibit radiosensitising effects in both lung cancer models tested, MMn demonstrated a radioprotective effect, and cisplatin (IV) demonstrated cytotoxic effects as a prodrug. These findings raise interesting questions for discussion regarding the mechanisms by which Texaphyrins and platinum (IV) work, namely.

- Does the presence of a Manganese core cause MMn to radioprotect by the depletion of ROS as opposed to the generation of it?
- Are platinum (IV) truly non-toxic prodrugs if cellular reducing agents can facilitate their reduction into active platinum (II)?
- Are platinum (IV) agents only effective when caged by another molecule that can facilitate their reduction in the correct environment?

Results II: POLQi

3.4 Validation of SHLD2 KO cell line

This project aimed to understand the mechanism behind POLQi-mediated radiosensitivity in SHLD2-disrupted cells, it was first important to validate the status of the SHLD2 gene in the cell line we were using by immunoblot (following the immunoblot protocol highlighted in section 2.6).

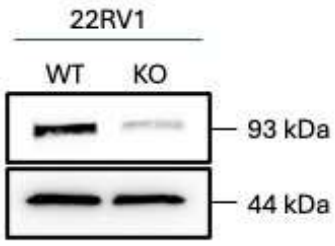

Figure 3.4.1 Immunoblot depicting the successful disruption of SHLD2 in the 22RV1 cell line. (Predicted MW of b-actin ~ 44 kDa, SHLD2~ 93 kDa).

KO cell lines are typically generated using Crispr-Cas9 technology. A single guide RNA (sgRNA) is synthesised to target the gene of interest, and the sgRNA forms a complex with the Cas protein. The sgRNA-Cas complex cleaves the DNA at the intended site on the genome, leading to DNA DSB by a DDR pathway such as NHEJ or HR. These repair mechanisms tend to introduce base insertions or deletions that can cause frameshift mutations, generating non-functional protein, hence generating a KO cell line (74). SHLD2 is considered an essential gene and, as a result, not only is the gene difficult to knock out, but it exists in two isoforms, Q86V20-1 and Q86V20-2. Therefore, alternative splicing could be the cause of the residual protein (75). Another reason could be mosaicism, where subpopulations of cells do not have SHLD2 knocked out and result in the presence of a faint band in the immunoblot. As SHLD2 was seen to be significantly disrupted, this was accepted as a SHLD2 disrupted cell line (referred to as SHLD2 KO).

3.5 Optimisation for the depletion of short-range resection factors using small-interfering RNA

To investigate the role of resection in POLQi-mediated radiosensitisation, it was first necessary to optimise a protocol for the consistent depletion of short-range resection factors, specifically MRE11 and CtIP. Achieving gene depletion with siRNA required us to optimise the siRNA concentration for this specific cell line. siNT was used at a concentration of 40 nM as a non-targeting control to account for transfection-associated toxicity. Based on the literature, 20 nM of siRNA was sufficient to achieve MRE11 knockdown (76). As a result, we initially tried 20 nM of siMRE11 and siCtIP, both of which were combined with 20 nM siNT to ensure all transfections used a total of 40 nM siRNA.

Whilst this concentration of siMRE11 seemed to offer some knockdown of the target gene, a significant proportion of the MRE11 protein remained (figure 3.4.1). This was especially noticeable in the 22RV1 SHLD2 KO. In contrast, knockdown with siCtIP was minimal,

confirming that these concentrations of siRNA were not sufficient to achieve gene knockdown.

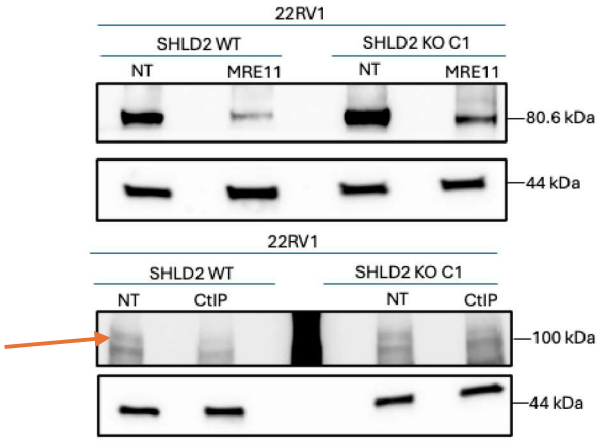

Figure 3.5.1 Immunoblots depicting the optimisation for the depletion of MRE11 and CtIP using their respective siRNA at 20 nM combined with 20 nM siNT to ensure all transfections had a total of 40 nM siRNA. Arrow indicates the 100 kDa band to show knockdown of CtIP. SiNT control was 40 nM. b-actin was used as a housekeeping gene (Predicted MW of b-actin ~ 44 kDa, MRE11 ~ 80.6 kDa, and CtIP ~100 kDa).

The incomplete knockdown warranted the use of greater siRNA concentrations. 40 nM of siMRE11, siCtIP and siNT demonstrated acceptable knockdown (Figure 3.4.2)

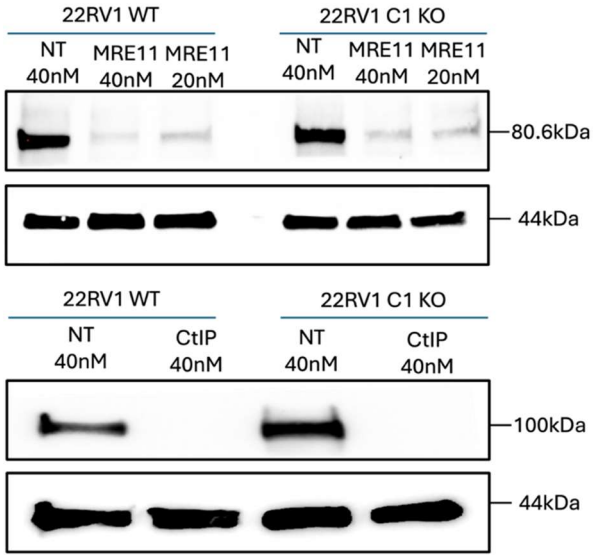

Figure 3.5.2 Immunoblots to validate the knockdown of 40nM siMRE11 and CtIP with 40nM of siNT still being used. b-actin was used as a housekeeping gene (Predicted MW of b-actin ~ 44 kDa MRE11 ~ 80.6 kDa and CtIP ~100 kDa).

3.6 Depletion of short-range resection factors fails to abrogate the POLQi-mediated radiosensitivity of SHLD2-disrupted 22RV1 cells

Following the siRNA concentration optimisation, both WT and SHLD2 KO cell lines had MRE11 and CtIP depleted by transfection with 40 nM siRNA (experimental details found in section 2.5). The transfected cells were then seeded and treated with 2μM ART558/DMSO before receiving a single fraction of 3 Gy radiation. We expect that depletion of MRE11 or CtIP would cause a reversal of the POLQi-mediated radiosensitisation in SHLD2-disrupted cells. The surviving fractions and related RPF are shown in tabulated form below (presented graphically in Figure 3.5.3)

Condition: 2 μM ART558	**SF of SHLD2 WT**		**RPF_{WT}**	**SF of SHLD2 KO**		**RPF_{KO}**
	DMSO	ART558		DMSO	ART558	
siNT	0.229	0.203	1.18	0.103	0.042	2.93
siMRE11	0.115	0.090	1.36	0.069	0.033	2.48
siCtIP	0.199	0.235	0.90	0.103	0.094	1.13

Condition: 4 μM ART558	**SF of SHLD2 WT**		**RPF_{WT}**	**SF of SHLD2 KO**		**RPF_{KO}**
	DMSO	ART558		DMSO	ART558	
siNT	0.212	0.188	1.13	0.090	0.031	3.01
siMRE11	0.104	0.088	1.24	0.071	0.031	2.34
siCtIP	0.154	0.163	0.94	0.094	0.057	1.69

Figure 3.6.1 Table summarising the numerical values of the SF and RPF depicted in figures 3.6.2 and 3.6.3. These values are used to make conclusions about the effect of short-range resection factor depletion on POLQi-mediated radiosensitisation.

SiNT was used as an experimental control to account for transfection-associated toxicity. Under this condition, it was expected that POLQi would not have any effect on the WT cell line but would cause radiosensitisation in the KO cell line. Mechanistically, this would be due to the

presence of SHLD2, which is thought to negatively regulate HR & MMEJ and positively regulate NHEJ through resection antagonism. Thus, when SHLD2 is present,
POLQi would have little effect as the drug targets a polymerase that's primarily active in MMEJ repair. However, when SHLD2 is disrupted, it's thought to induce a hyper-resection phenotype in the cell, increasing the amount of MMEJ such that POLQi has a greater radiosensitising effect.

At 2 μM, RPF_{WT} and RPF_{KO} for the control condition were significantly different, indicating the SHLD2 KO cell line is sensitive to POLQi with radiation.. At 4 μM, we see an increased level of radiosensitisation indicated by the increased RPF_{KO} of 3.01 (compared to 2.93 in the 2 μM experimental arm). This confirmed a greater concentration of ART558 caused a greater radiosensitisation in the KO cell line. As such, siNT's RPF_{KO} was used as a comparative baseline for the other experimental conditions to assess the reversal of radiosensitivity in both experimental arms.

If the hypothesis of Project II holds, and POLQi-mediated radiosensitisation is governed by DNA end resection, then the depletion of MRE11 or CtIP should yield a reversal of the radiosensitisation seen in the siNT KO cell line. Following the depletion of MRE11, the difference in RPF_{WT} and RPF_{KO} remained significant ($p = 0.0024$), implying that 2 μM ART558 was still radiosensitising the KO cell line. The MRE11 depletion continued to have no effect on POLQi-mediated radiosensitivity at an increased POLQi concentration. Whilst the RPF_{KO} was significantly less than that of the NT control ($p=0.0007$), the difference in SF between the DMSO and POLQi treatment groups also remained significant, indicating that ART558 had still radiosensitised the SHLD2-disrupted cells.

In contrast, when CtIP was depleted, the difference in RPF_{WT} and RPF_{KO} was minimal and statistically insignificant ($p=0.4496$). Additionally, the RPF_{KO} of the siCtIP condition was

significantly less than that of the NT control, suggesting that depletion of CtIP had abrogated POLQi-mediated radiosensitisation at this concentration of inhibitor. However, in the 4 μM concentration the difference between the SF of DMSO and POLQi treatment groups was significant (p=0.0003). Thus, it is clear that ART558 is still exerting a radiosensitising effect but just to a lesser extent that that of the NT control.

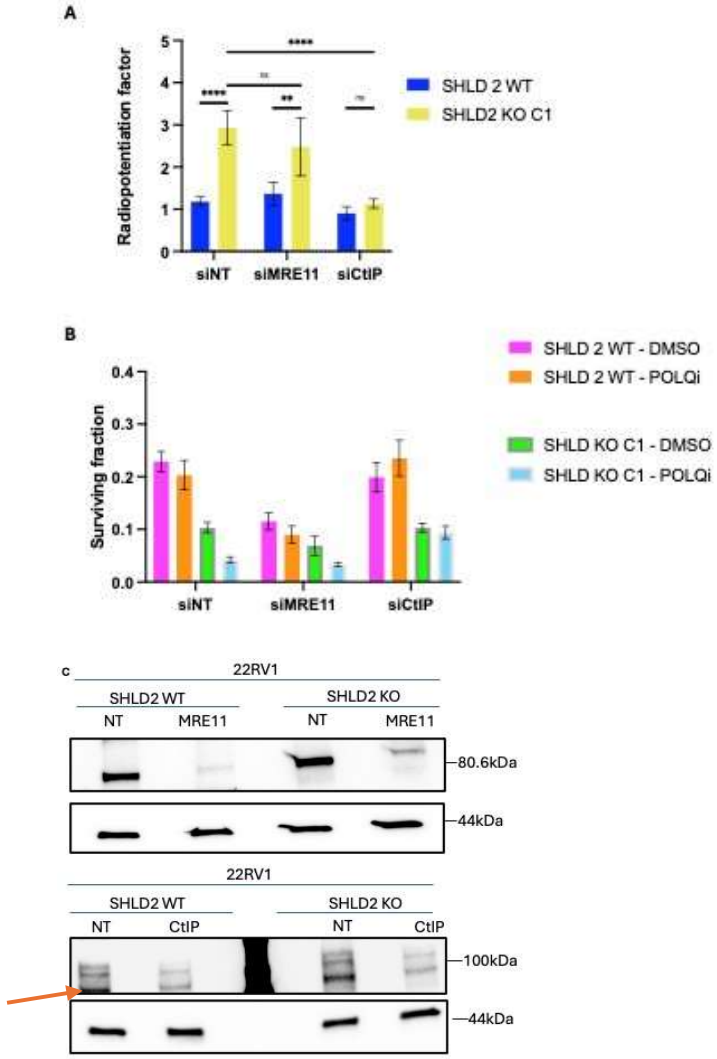

Figure 3.6.2 (A) Bar graph illustrating the difference in radiopotentiation factor between 22RV1 WT and SHLD2 KO, where radiopotentiation factor = surviving fraction (DMSO)/surviving fraction (ART558) (n=3). Analysed by 2-way ANOVA with ad-hoc Tukey's corrections (ns, not significant, **, P<0.01, ****, P<0.0001). **(B)** Representative bar charts indicating the surviving fractions of 22RV1 WT and SHLD2 KO when treated with 2 μM ART558, these values were used to calculate the radiopotentiation factor (RPF) (n=3). **(C)** Immunoblots showing that transfection with 40 nM siRNA achieved knockdown of short-range resection factors. Arrow indicates the 100 kDa band to show knockdown of CtIP (Predicted MW of b-actin ~ 44 kDa MRE11 ~ 80.6 kDa and CtIP ~100 kDa)

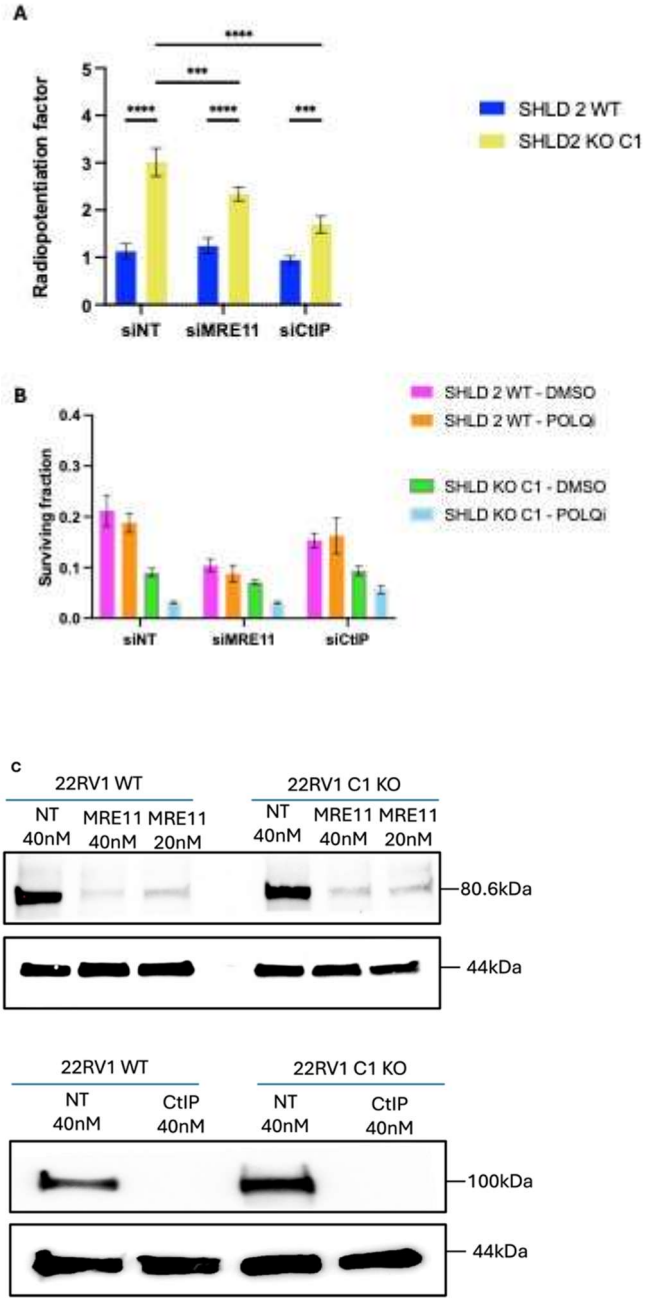

Figure 3.6.3 (A) Bar graph illustrating the difference in radiopotentiation factor between 22RV1 WT and SHLD2 KO, where radiopotentiation factor = surviving fraction (DMSO)/surviving fraction (ART558) (n=3). Analysed by 2-way ANOVA with ad-hoc Tukey's corrections (***, P<0.001, ****, P<0.0001). **(B)** Representative bar charts indicating the surviving fractions of 22RV1 WT and SHLD2 KO when treated with 4 μM ART558, these values were used to calculate the radiopotentiation factor (RPF) (n=3). **(C)** Immunoblots showing that transfection with 40 nM siRNA achieved knockdown of short-range resection factors. (Predicted MW of b-actin ~ 44 kDa MRE11 ~ 80.6 kDa and CtIP ~100 kDa)

In the context of our original hypothesis, the data reveals some unexpected findings. Specifically, MRE11 does not appear to be involved in POLQi-mediated radiosensitisation of SHLD2-disrupted cells, while CtIP seems to play a partial role at lower inhibitor concentrations, with less involvement at higher concentrations. These results raise the following questions for discussion.

- Does knockdown of MRE11 or CtIP lead to a full loss of resection in the cell?
- Are there alternative resection factors involved that are capable of initiating resection in the absence of MRE11/CtIP?
- Assuming resection loss is complete with MRE11/CtIP depletion, is there a POLQdependent, resection-independent mechanism that is affected?

Chapter 4: Discussion

Discussion I - MangaCisTEX

4.1 Summary of Findings I

This half of the thesis explored a novel Texaphyrin compound, MMn, as well as a cisplatin (IV) agent, noting their effects as single agents and when chemically conjugated to form MangaCisTEX. MMn is thought to be a tumour-accumulating redox cycler that can induce oxidative stress in the cell but also reduce inactive cisplatin (IV) into its active, toxic form, cisplatin (II). Therefore, when the two are conjugated to form MangaCisTEX, this project hypothesised that the conjugate would provide tumour radiosensitisation of *in vitro* lung cancer models. In both models (H1299 and A549), MangaCisTEX was unexpectedly shown to demonstrate dose-dependent cytotoxicity independent of radiation. When further investigations were carried out into the constituent molecules that make up the compound, more unexpected results were seen. The Texaphyrin was seen to exert radioprotective effects, and the prodrug cisplatin (IV) demonstrated cytotoxicity. This challenges the traditional mechanisms that Texaphyrins and platinum (IV) agents were thought to work by. In this chapter, I will discuss how the results of this project fit the research of others in the same field and propose new directions for this field of work.

4.2 Challenging the mechanisms of Texaphyrins and platinum (IV) agents

Texaphyrins were first conceptualised in 1988, and their clinical applications became very apparent at the turn of the 21st century (19,77). MGd was one of the first Texaphyrins to be developed and showed very promising results *in vitro*, however, when put into phase III clinical trials as a clinical radiosensitiser, it failed to significantly impact patient survival and, as a result, was not approved by the FDA (19,25). When tested in this series of experiments, MGd was unable to cause a statistically significant radiosensitisation. Structurally, the difference between MGd and MMn is the replacement of a Gd (III) core with an Mn (II) one, but mechanistically, the propagation of redox reactions and generation of ROS was not expected to change between both Texaphyrin compounds.

Structurally, MGd is a Gd (III) core encaged by a Texaphyrin ring, which acts as a chelating agent to prevent the release of Gd^{3+} ions into the cellular environment that cause toxicity by competing with other endogenous ions such as Ca^{2+} in important biological processes (78). The MGd molecule generates ROS by firstly oxidising cellular metabolites such as NADPH and then, when in the reduced conformation, reducing cellular oxygen to form ROS species such as superoxide or hydrogen peroxide. Throughout this futile redox cycling process, the Gd core remains stabilised in the 3+ oxidation state (20,78,79). However, a potential reason for the difference in cell viability data between MGd and MMn may lie in the chemistry of oxidation states. Mn can exist in oxidation states -3 to +7 (i.e. it can gain three electrons or lose seven to gain a stable outer shell) (80). For this reason, Manganese has been incorporated into other molecules, such as nanozymes or porphyrins, to form ROS-scavenging biomaterials. The basis of this is due to Mn's biological activity when bound to superoxide dismutase (MnSOD).

MnSOD is a mitochondrial enzyme that catalyses the dismutation of superoxide into cellular oxygen and hydrogen peroxide (which is further broken down by catalase into water and oxygen) (81). Essentially, the variable oxidation states of Mn mean that MnSOD can bind superoxide when Mn is in the 3+ state and the transition metal accepts an electron, leading to the generation of cellular oxygen, leaving the Mn to temporarily exist in the 2+ state (illustrated in figure 4.2.1).

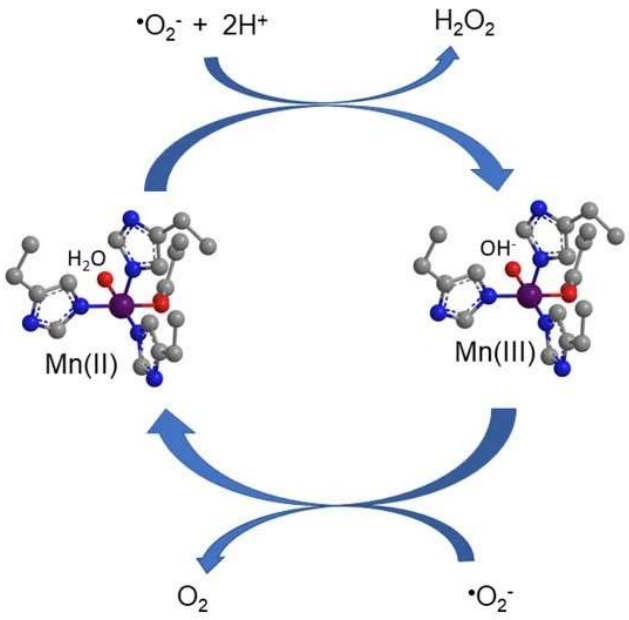

Figure 4.2.1 Schematic depicting the variable oxidation states of Mn in MnSOD and how this contributes to the reduction of superoxide (O_2^-) and the generation of hydrogen peroxide (H_2O_2) as a substrate for catalase. This figure is from Rouco et al., 2020.

Mn can then donate this electron back to another superoxide molecule to form hydrogen peroxide, which is later catalysed by catalase (83). The variable oxidation states of Mn in this scenario allow the dismutase to scavenge ROS and exhibit antioxidant effects within the mitochondria. During the development of MGd, a manganese-texaphyrin was characterised, and it has been shown that the compound can act as an oxidation catalyst for ascorbate and generate ROS in a similar way to MGd. However, it may be possible that Mn's variable oxidation state contributes to MMn's ability to scavenge ROS and, therefore, when placed as the core of a Texaphyrin in MMn, cause the observed radioprotection (79,84). MMn is relatively novel, and its radioprotective effect has not been observed elsewhere, but Mn porphyrins (Texaphyrins are expanded classes of porphyrins) like Mn (III) *meso*-tetrakis (N-n-hexylpyridinium-2-yl) Porphyrin (MnTnHex-2PyP^{5+}) has shown robust *in vivo* radioprotective effects in the pulmonary tissue of Fischer344 rats by scavenging ROS (85). At best, this could suggest a repurposing of MMn as a radioprotective agent administered to healthy tissue, but at worst, MMn is an

ineffective generator of ROS and further work involving this Texaphyrin should not be continued.

Another unexplained observation from the findings of this thesis was the cytotoxicity of a purported non-toxic prodrug, cisplatin (IV). When tested, unirradiated cells treated with increasing concentrations of cisplatin (IV) demonstrated a reduction in their viability. Radiation had no additive effect on this cell killing, and the amount of cell killing was less than that of the cisplatin (II) treated cells. The toxicity of platinum (IV) drugs has also been noted in the work of other groups. A very recently published study aimed to characterise radiobiological hypoxia (<0.1% oxygen) as an activating factor for fluorogenic platinum (IV) compounds. The fluorogenic cisplatin (IV) molecule (CisNap) was shown to exhibit toxicity, even at normoxic conditions, with 5 μM of CisNap demonstrating a 100% reduction in the A549 surviving fraction (as measured by colony formation assay) (86). The level of cisplatin (IV) cytotoxicity seen in that work was significantly greater than the observed effects in this work. The variation in cisplatin (IV) cytotoxicity between various groups could signify a lack of stability in this molecule, likely suggesting the spontaneous reduction of cisplatin (IV) occurs when used as a single agent, causing variable toxicity.

Our result was unexpected, as platinum (IV) agents were thought to be inactive due to the stable octahedral conformation they adapt, which reduces the rate of aquation and subsequent activation (87). However, a chemical study using NMR spectroscopy and flameless atomic absorbance spectroscopy (FAAS) uncovered that asymmetric Pt(IV) compounds, such as our cisplatin (IV), can be reduced to their active Pt(II) form in the presence of light (photoreduction) (88). Whilst we tried to mitigate the drug's light sensitivity and protect its stock and assay plates from light, it is highly unlikely every measure can be taken to eliminate the presence of light. It is possible to use ^{1}H NMR spectroscopy to assess the effect of light on the compound's activity. If we hypothesise that light causes the platinum (IV) to lose the two axial ligands holding it in an octahedral

conformation and revert it to its platinum (II) state as a square planar molecule (illustrated in Figure 4.2.2), then this would be confirmed by a chemical shift in proton resonance.

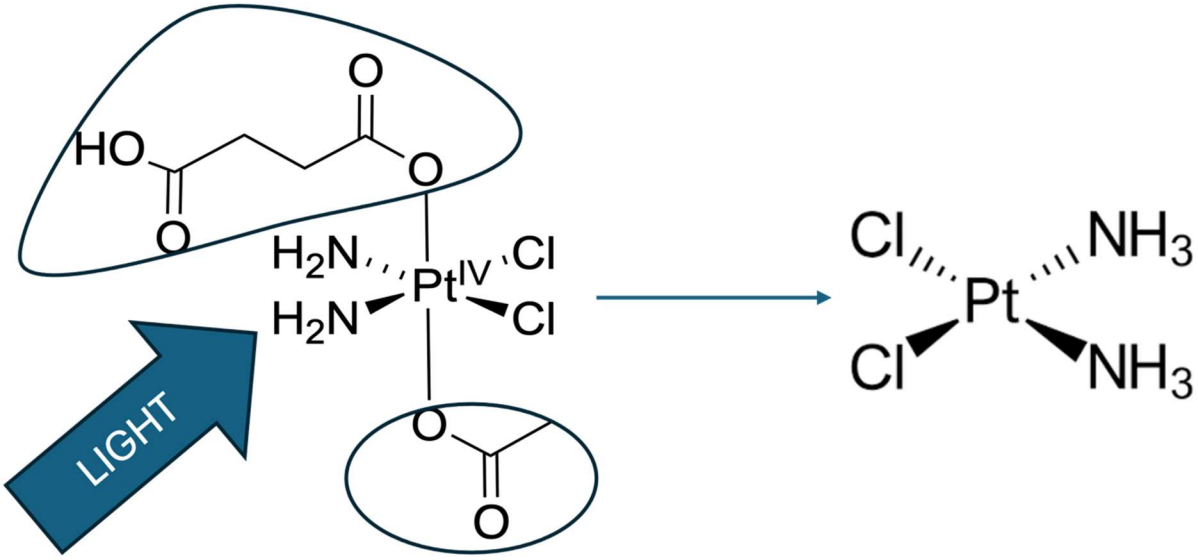

Figure 4.2.2 Schematic image depicting the loss of the (circled) axial ligands in the presence of light reducing an octahedral cisplatin (IV) to a square planar cisplatin (II).

The propensity of platinum (IV) to be spontaneously reduced by light and other biological reducing agents is rather contradictory to its proposed mechanism of action. In order to overcome this and fully utilise the “non-toxic” properties of these agents, the use of photoremovable protecting groups as a molecular caging method is imperative.

4.3 Limitations of Project I

When looking for the potential clinical applications of Texaphyrin-Platinum (IV) conjugates, it is typically assessed as a tumour-specific radiosensitiser. Whilst this work only assessed the ability of MangaCisTEX to augment cell killing in the presence of radiation, the next steps would be to characterise its full function as a tumour-specific radiosensitising agent. Whilst a normal human cell line could have been introduced (such as MRC5), the fundamental limitation lies within the use of 2D tissue culture to assess the compound. Should this work be continued looking to truly assess MangaCisTEX as a

radiosensitising agent, it is recommended that some 3D techniques be implemented, such as the use of organoids or perhaps the use of *in vivo* research techniques.

4.4 Conclusion and Future Perspectives I

Whilst the Texaphyrin-Platinum (IV) conjugate may have failed, I believe there is still merit in each of the constituent compounds. Whilst MMn's ability to efficiently generate ROS has been called into question, if the effect is due to the Mn (II) core, as explained, then it is still possible to trial novel Texaphyrins with different transition metal cores.

The ingenuity of platinum (IV) agents is the ability to take a platinum (II) core and add two axial ligands (circled in Figure 4.2.2) that make it more stable and can offer some form of targeting. Whilst the axial ligands can include things like hydroxyl groups or more acetates that stabilise the molecule without adding biological function, it is also possible to add other cytotoxic agents, molecular guiding molecules or enzyme inhibitors to boost function (89). Dual-platinum (IV) agents such as Mitaplatin are composed of a cisplatin (II) backbone and two dichloroacetate (DCA) ligands. DCA acts as a pyruvate dehydrogenase kinase, shifting the metabolic pathway of the cancer cell and leading to Cas-mediated cell death (90,91). When combined with the DNA adducts cisplatin generates, mitaplatin has shown *in vitro* potency when tested in hepatoma cell lines (92).

The avenues into exploring Texaphyrins and platinum (IV) compounds as anticancer agents are ever increasing, and perhaps when their mechanisms of action are more understood, the concept of Texaphyrin-Platinum (IV) conjugates as radiosensitisers should be revisited.

Discussion II: POLQi

4.5 Summary of Findings II

This half of the thesis explored an established radiosensitising agent, ART558 and how it mediates radiosensitisation in SHLD2-disrupted cells. Using an *in vitro* prostate cancer model, we hypothesised that if resection is the mechanism behind POLQi-mediated radiosensitisation, then the depletion of MRE11 or CtIP should reverse or “rescue” radiosensitivity. Two concentrations of POLQi were tested, 2 μM and 4 μM, for which we could conclude that MRE11 depletion does not abrogate POLQi-mediated radiosensitivity. However, CtIP depletion was able to abrogate POLQi-mediated radiosensitivity at 2 μM ART558 but not at 4 μM ART558. This section will aim to discuss these findings in the context of what is already known in the field, as well as suggest future avenues for scientific exploration.

4.6a – Synthetic lethality of POLQ inhibition and 53BP1 defects

53BP1 is a protein that antagonises resection, and whilst its definitive mechanism of action remains unknown, it is thought to exact this effect through the shieldin complex. A cellular study conducted by Zatreanu et al. used a siRNA designed to target SHLD2, and when knocked down, RPE-1 cells conferred profound sensitivity to treatment with POLQi. The same was true for a siRNA targeting REV7 (another subunit of the shieldin complex), causing profound POLQi sensitivity (67). This confirmed a synthetic lethality between defects in 53BP1 (as tested by the knockdown of two critical subunits of 53BP1’s effector molecule) and POLQ inhibition. The results of this work implicated resection factors in the mechanism of action of this POLQi-mediated sensitivity, and the work of this thesis assessed short-range resection factors MRE11 and CtIP as they are canonically believed to initiate DNA end resection (53,93).

4.6b Short-resection and POLQi-mediated radiosensitisation

The findings of this thesis raised three fundamental questions for discussion.

- Is resection loss complete with the knockdown of MRE11 or CtIP?
- Are there alternative nucleases involved that are capable of performing resection in the absence of these two molecules?
- Assuming resection is impaired following the depletion of these resection factors, is there a POLQ-dependent, resection-independent mechanism of repair responsible for the residual POLQi-mediated radiosensitivity observed?

Whilst 2 μM of ART558 radiosensitised the SHLD2 KO cell line (RFP of 2.90), it was clear from the data that 4 μM of the inhibitor elicited a slightly stronger radiosensitisation (RPF of 3.01), the difference in which may contain the reason as to why we saw CtIP rescue radiosensitivity at 2 μM but not at 4 μM ART558. Interestingly, at the lower inhibitor concentration, MRE11 depletion was still unable to abrogate the radiosensitising effect of ART558. When considering the results of the 4 μM experimental arm, CtIP depletion is unable to abrogate the radiosensitising effect of ART558 also, perhaps suggesting a method of POLQ-dependent repair that doesn't involve MRE11 or CtIP. A molecular study performed by Tomimatsu et al. utilised live-cell imaging techniques with subsequent BrdU foci quantification in 1BR3 WT cells to study end-resection (23). Replication protein A (RPA) was fluorescently tagged with green fluorescent protein (GFP) to form GFP-RPA, allowing the group to study resection kinetics by visualising the accumulation of GFPRPA. When MRE11 or CtIP were depleted, GFP-RPA accumulation was reduced, but maximum accumulation was still reached just after 120 minutes. This suggested that in the absence of MRE11 or CtIP, resection still occurs but at a slower rate. Following the ablation of EXO1 on top of MRE11 or CtIP depletion, resection was severely impaired, pointing towards EXO1 being a major player in resection when MRE11 or CtIP are absent. Relating to our findings, the presence of POLQi-mediated radiosensitisation in the

absence of short-range resection factors could be a result of EXO1 continuing to propagate resection as a backup pathway.

Another theory that may explain the residual POLQi radiopotentiation is the presence of a POLQ-dependent, resection-independent repair mechanism such as translesion synthesis (TLS). IR induces cellular damage by various mechanisms, such as the generation of abasic sites and thymine glycol lesions (95). TLS is a DNA damage tolerance mechanism that is designed to reduce the amount of stalled replication forks, thus reducing replicative stress (96). POLQ has been implicated as a polymerase used in TLS for over two decades due to its ability to bypass abasic sites and thymine glycol lesions. However, the specific regions of the protein involved in this ability have recently been uncovered. POLQ's catalytic domain contains three inserted motifs: the R2254 motif of the second insert, as well as tyrosine residue 2387/2391 in the finger subdomain, and these have been shown to be critical for POLQ's unique ability to bypass abasic sites (97–99). POLQ is also able to bypass thymine glycol lesions by preferentially incorporating deoxyadenosine monophosphate (dAMP). *In vitro* experiments where POLQ was knocked out demonstrated both reduced fork activity and increased frequency of fork stalling (96,100).

Linking this back to the findings of this thesis, our use of gamma irradiation causes various clustered DNA lesions where DSB, SSB, abasic sites and other forms of damage are all located within two turns of the DNA helix (101). Abasic sites are often formed through the radiolysis of water, creating hydroxyl radicals which attack the glycosidic bond between base and pentose sugar (102). Thymine glycol lesions are another result of hydroxyl radicals attacking the double bonds in thymine and incorporating themselves into the base, forming 5,6-dihydroxy-5,6-dihydrothymine or thymine glycol (103). Both abasic sites and thymine glycol are mutagenic and highly disturbing to replicative polymerases.

Therefore, following radiation's induction of DNA clustered lesions such as those above, POLQ's ability to extend and prime over these become essential to maintaining the velocity of the replication fork and subsequent DNA repair. Therefore, whilst depletion of MRE11 or CtIP may have impacted resection and, as a result, reversed POLQi-mediated radiosensitisation, it is also possible the residual radiopotentiation caused by ART558 was due to the inhibitor's effects on POLQ when it was active in TLS following gamma irradiation.

4.7 Limitations of Project II

The use of siRNA is a widely used experimental technique to knock down specific genes *in vitro,* and the result of validation immunoblots confirms that MRE11 and CtIP were indeed knocked down with 40 nM of siRNA. However, a more robust method directly showing how MRE11 or CtIP depletion affects DNA end resection, for example, BrdU foci imaging, an AsISI assay or an MMEJ reporter. This would have been beneficial to clarify what resection factor(s) need to be knocked down to significantly affect the amount of resection and, therefore, MMEJ. Additionally, we were limited to siRNA knockdowns of these factors therefore, knocking down multiple resection factors would have introduced transfection-associated toxicity. Should we have had MRE11/CtIP knockout cell lines, we could have validated our results and possibly looked into the combined effect of also knocking down other resection factors like EXO1, BLM, WRN or DNA2.

4.8 Conclusion and Future Perspectives II

The results of this thesis indicate further investigation into the effects of DNA resection and its role in POLQi-mediated radiosensitisation is still needed. Therefore, if we understand the link between DNA end resection and the effects of POLQi, it is possible that patients could be screened for SHLD2 status as a stratification method for treatment with POLQi and RT.

4.9 Concluding remarks

Radioresistance remains a major hindrance to the efficacy of RT as a clinical treatment. Evaluating both novel and repurposed compounds as radiosensitisers is essential for improving patient outcomes whilst minimising adverse effects and helping to avoid more aggressive treatment options. This thesis has revealed a promising avenue of investigation in exploring how DNA resection influences POLQ inhibition-mediated radiosensitivity, particularly in SHLD2-disrupted cells. This line of research holds significant potential and may ultimately warrant further in vivo studies, with the goal of progressing to clinical trials aimed at stratifying patients for treatment with POLQi and RT.

References:

1. Cooper GM. The Development and Causes of Cancer. In: The Cell: A Molecular Approach 2nd edition [Internet]. Sinauer Associates; 2000 [cited 2024 Jul 3]. Available from: https://www.ncbi.nlm.nih.gov/books/NBK9963/

2. Hassanpour SH, Dehghani M. Review of cancer from perspective of molecular. Journal of Cancer Research and Practice. 2017 Dec 1;4(4):127–9.

3. Baskar R, Lee KA, Yeo R, Yeoh KW. Cancer and Radiation Therapy: Current Advances and Future Directions. Int J Med Sci. 2012 Feb 27;9(3):193–9.

4. Chaput G, Regnier L. Radiotherapy. Can Fam Physician. 2021 Oct;67(10):753–7.

5. Spencer K, Parrish R, Barton R, Henry A. Palliative radiotherapy. BMJ. 2018 Mar 23;360:k821.

6. Borrego-Soto G, Ortiz-López R, Rojas-Martínez A. Ionizing radiation-induced DNA injury and damage detection in patients with breast cancer. Genet Mol Biol. 2015;38(4):420–32.

7. Types of radiotherapy | The Royal Marsden [Internet]. [cited 2024 Jul 9]. Available from: https://www.royalmarsden.nhs.uk/your-care/treatments/radiotherapy/types-radiotherapy

8. Steel GG. The 5Rs of Radiobiology. Int J Radiat Biol. 2009 Jul 3;(6):1045–8.

9. Juan C Alamilla-Presuel, Antonio M Burgos-Molina, Alejandro González-Vidal, Francisco Sendra-Portero, Miguel J Ruiz-Gómez. Factors and molecular mechanisms of radiation resistance in cancer cells. Int J Radiat Biol. 2022 Feb 22;98(8):1301–15.

10. Schulz A, Meyer F, Dubrovska A, Borgmann K. Cancer Stem Cells and Radioresistance: DNA Repair and Beyond. Cancers (Basel). 2019 Jun 21;11(6):862.

11. Cao K, Chen Y, Zhao S, Huang Y, Liu T, Liu H, et al. Sirt3 Promoted DNA Damage Repair and Radioresistance Through ATM-Chk2 in Non-small Cell Lung Cancer Cells. J Cancer. 2021 Jul 13;12(18):5464–72.

12. Zhang J, Xiang H, Liu J, Chen Y, He RR, Liu B. Mitochondrial Sirtuin 3: New emerging biological function and therapeutic target. Theranostics. 2020 Jul 9;10(18):8315–42.

13. Wohlhueter RM, McIvor RS, Plagemann PG. Facilitated transport of uracil and 5-fluorouracil, and permeation of orotic acid into cultured mammalian cells. J Cell Physiol. 1980 Sep;104(3):309–19.

14. Longley DB, Harkin DP, Johnston PG. 5-Fluorouracil: mechanisms of action and clinical strategies. Nat Rev Cancer. 2003 May;3(5):330–8.

15. Kaur J, Marcus S, Garg S, Kansal A. Redefining Role of 5-Fluorouracil and Exploring the Impact of Taxanes and Cisplatin in Locally Advanced and Recurrent Carcinoma Cervix in Concurrent Setting With Radiotherapy: A Literature Review. Cureus. 12(11):e11645.

16. Saint A, Evesque L, Falk AT, Cavaglione G, Montagne L, Benezery K, et al. Mitomycin and 5fluorouracil for second-line treatment of metastatic squamous cell carcinomas of the anal canal. Cancer Med. 2019 Sep 16;8(16):6853–9.

17. Gad SE. Mitomycin C. In: Wexler P, editor. Encyclopedia of Toxicology (Third Edition). Oxford: Academic Press; 2014. p. 354–6.

18. Rosenthal DI, Fuller CD, Machtay M, Algazy KM, Meyer DM, Kaiser LR, et al. Phase I Study of Paclitaxel Given by Seven-Week Continuous Infusion Concurrent with Radiation Therapy for Locally Advanced Non–Small Cell Lung Cancer. Journal of Thoracic Oncology. 2006 Jan 1;1(1):38–45.

19. Sessler JL, Miller RA. Texaphyrins: new drugs with diverse clinical applications in radiation and photodynamic therapy. Biochem Pharmacol. 2000 Apr 1;59(7):733–9.

20. Magda D, Lepp C, Gerasimchuk N, Lee I, Sessler JL, Lin A, et al. Redox cycling by motexafin gadolinium enhances cellular response to ionizing radiation by forming reactive oxygen species. Int J Radiat Oncol Biol Phys. 2001 Nov 15;51(4):1025–36.

21. Wu J. The Enhanced Permeability and Retention (EPR) Effect: The Significance of the Concept and Methods to Enhance Its Application. J Pers Med. 2021 Aug 6;11(8):771.

22. Lugano R, Ramachandran M, Dimberg A. Tumor angiogenesis: causes, consequences, challenges and opportunities. Cell Mol Life Sci. 2019 Nov 6;77(9):1745–70.

23. Maloney JP, Gao L. Proinflammatory Cytokines Increase Vascular Endothelial Growth Factor Expression in Alveolar Epithelial Cells. Mediators Inflamm. 2015;2015:387842.

24. Leu AJ, Berk DA, Lymboussaki A, Alitalo K, Jain RK. Absence of functional lymphatics within a murine sarcoma: a molecular and functional evaluation. Cancer Res. 2000 Aug 15;60(16):4324–7.

25. Mehta MP, Shapiro WR, Phan SC, Gervais R, Carrie C, Chabot P, et al. Motexafin Gadolinium Combined With Prompt Whole Brain Radiotherapy Prolongs Time to Neurologic Progression in Non–Small-Cell Lung Cancer Patients With Brain Metastases: Results of a Phase III Trial. International Journal of Radiation Oncology*Biology*Physics. 2009 Mar 15;73(4):1069–76.

26. Oun R, Moussa YE, Wheate NJ. The side effects of platinum-based chemotherapy drugs: a review for chemists. Dalton Trans. 2018 May 15;47(19):6645–53.

27. Latif LA, Eaborn C, Pidcock AP, Weng NS. Square planar platinum(II) complexes. Crystal structures of *cis*-bis(triphenylphosphine)hydro (triphenylstannyl)platinum(II) and *cis*bis(triphenylphosphine)hydro(triphenylsilyl)platinum(II). Journal of Organometallic Chemistry. 1994 Jul 12;474(1):217–21.

28. Alcindor T, Beauger N. Oxaliplatin: a review in the era of molecularly targeted therapy. Curr Oncol. 2011 Feb;18(1):18–25.

29. Zhang C, Xu C, Gao X, Yao Q. Platinum-based drugs for cancer therapy and anti-tumor strategies. Theranostics. 2022 Feb 7;12(5):2115–32.

30. Hashimoto S, Anai H, Hanada K. Mechanisms of interstrand DNA crosslink repair and human disorders. Genes and Environment. 2016 May 1;38(1):9.

31. Tang J, Zhao L. Preparation of DNA interstrand cross-link repair intermediates induced by abasic sites. MethodsX. 2022 Apr 6;9:101687.

32. Ben-Yehoyada M, Wang LC, Kozekov ID, Rizzo CJ, Gottesman ME, Gautier J. Checkpoint signaling from a single DNA interstrand crosslink. Mol Cell. 2009 Sep 11;35(5):704–15.

33. Deans AJ, West SC. DNA interstrand crosslink repair and cancer. Nat Rev Cancer. 2011 Jul;11(7):467–80.

34. Wang Z, Deng Z, Zhu G. Emerging platinum(IV) prodrugs to combat cisplatin resistance: from isolated cancer cells to tumor microenvironment. Dalton Trans. 2019 Feb 19;48(8):2536–44.

35. Wang Z, Zhu G. DNA Damage Repair Pathways and Repair of Cisplatin-Induced DNA Damage. In: Reference Module in Chemistry, Molecular Sciences and Chemical Engineering [Internet]. Elsevier; 2018 [cited 2024 Oct 6]. Available from: https://www.sciencedirect.com/science/article/pii/B9780124095472142519

36. Ienco A, Ruffo F, Manca G. The Role of Inverted Ligand Field in the Electronic Structure and Reactivity of Octahedral Formal Platinum (IV) Complexes. Chemistry – A European Journal. 2023;29(59):e202301669.

37. Arambula JF, Sessler JL, Siddik ZH. A texaphyrin–oxaliplatin conjugate that overcomes both pharmacologic and molecular mechanisms of cisplatin resistance in cancer cells. Medchemcomm. 2012;3(10):1275–81.

38. Brown A, Kumar S, Tchounwou PB. Cisplatin-Based Chemotherapy of Human Cancers. J Cancer Sci Ther. 2019;11(4):97.

39. Cox J, Graham Y. Gadolinium use and risks: an update for colleagues in primary care. Br J Gen Pract. 2021 Oct 1;71(711):444–5.

40. Blomqvist L, Nordberg GF, Nurchi VM, Aaseth JO. Gadolinium in Medical Imaging—Usefulness, Toxic Reactions and Possible Countermeasures—A Review. Biomolecules. 2022 May 24;12(6):742.

41. Ye Z, Shi Y, Lees-Miller SP, Tainer JA. Function and Molecular Mechanism of the DNA Damage Response in Immunity and Cancer Immunotherapy. Front Immunol [Internet]. 2021 Dec 14 [cited 2024 Oct 10];12. Available from: https://www.frontiersin.org/journals/immunology/articles/10.3389/fimmu.2021.797880/full

42. Huang RX, Zhou PK. DNA damage response signaling pathways and targets for radiotherapy sensitization in cancer. Sig Transduct Target Ther. 2020 May 1;5(1):1–27.

43. Wyatt DW, Feng W, Conlin MP, Yousefzadeh MJ, Roberts SA, Mieczkowski P, et al. Essential roles for Polymerase θ mediated end-joining in repair of chromosome breaks. Mol Cell. 2016 Aug 18;63(4):662–73.

44. Rodgers K, McVey M. Error-prone repair of DNA double-strand breaks. J Cell Physiol. 2016 Jan;231(1):15–24.

45. Mateos-Gomez PA, Gong F, Nair N, Miller KM, Lazzerini-Denchi E, Sfeir A. Mammalian polymerase θ promotes alternative NHEJ and suppresses recombination. Nature. 2015 Feb;518(7538):254–7.

46. McVey M, Lee SE. MMEJ repair of double-strand breaks (director's cut): deleted sequences and alternative endings. Trends Genet. 2008 Nov;24(11):529–38.

47. Lee NS, Kim S, Jung YW, Kim H. Eukaryotic DNA damage responses: Homologous recombination factors and ubiquitin modification. Mutat Res. 2018 May;809:88–98.

48. Mah LJ, El-Osta A, Karagiannis TC. γH2AX: a sensitive molecular marker of DNA damage and repair. Leukemia. 2010 Apr;24(4):679–86.

49. Bian L, Meng Y, Zhang M, Li D. MRE11-RAD50-NBS1 complex alterations and DNA damage response: implications for cancer treatment. Molecular Cancer. 2019 Nov 26;18(1):169.

50. You Z, Bailis JM. DNA damage and decisions: CtIP coordinates DNA repair and cell cycle checkpoints. Trends Cell Biol. 2010 Jul;20(7):402–9.

51. Kciuk M, Gielecińska A, Mujwar S, Mojzych M, Kontek R. Cyclin-dependent kinases in DNA damage response. Biochimica et Biophysica Acta (BBA) - Reviews on Cancer. 2022 May 1;1877(3):188716.

52. Setiaputra D, Durocher D. Shieldin – the protector of DNA ends. EMBO reports. 2019 May;20(5):e47560.

53. Zhao F, Kim W, Kloeber JA, Lou Z. DNA end resection and its role in DNA replication and DSB repair choice in mammalian cells. Exp Mol Med. 2020 Oct;52(10):1705–14.

54. Krejci L, Altmannova V, Spirek M, Zhao X. Homologous recombination and its regulation. Nucleic Acids Res. 2012 Jul;40(13):5795–818.

55. Stinson BM, Loparo JJ. Repair of DNA Double-Strand Breaks by the Non-homologous End Joining Pathway. Annu Rev Biochem. 2021 Jun 20;90:137–64.

56. Mirman Z, Lottersberger F, Takai H, Kibe T, Gong Y, Takai K, et al. 53BP1-RIF1-shieldin counteracts DSB resection through CST- and Polα-dependent fill-in. Nature. 2018 Aug;560(7716):112–6.

57. Tomida J, Takata K, Bhetawal S, Person MD, Chao H, Tang DG, et al. FAM35A associates with REV7 and modulates DNA damage responses of normal and BRCA1-defective cells. The EMBO Journal. 2018 Jun 15;37(12):e99543.

58. Fackrell K, Bobins L, Parul, Tomida J. FAM35A/SHLD2/RINN2: A novel determinant of double strand break repair pathway choice and genome stability in cancer. Environmental and Molecular Mutagenesis. 2020;61(7):709–15.

59. Ramsden DA, Carvajal-Garcia J, Gupta GP. Mechanism, cellular functions and cancer roles of polymerase-theta-mediated DNA end joining. Nat Rev Mol Cell Biol. 2022 Feb;23(2):125–40.

60. Black SJ, Ozdemir AY, Kashkina E, Kent T, Rusanov T, Ristic D, et al. Molecular basis of microhomology-mediated end-joining by purified full-length Polθ. Nat Commun. 2019 Sep 27;10(1):4423.

61. Ceccaldi R, Liu JC, Amunugama R, Hajdu I, Primack B, Petalcorin MIR, et al. Homologousrecombination-deficient tumours are dependent on Polθ-mediated repair. Nature. 2015 Feb;518(7538):258–62.

62. Kent T, Chandramouly G, McDevitt SM, Ozdemir AY, Pomerantz RT. Mechanism of microhomology-mediated end-joining promoted by human DNA polymerase θ. Nat Struct Mol Biol. 2015 Mar;22(3):230–7.

63. Koole W, van Schendel R, Karambelas AE, van Heteren JT, Okihara KL, Tijsterman M. A Polymerase Theta-dependent repair pathway suppresses extensive genomic instability at endogenous G4 DNA sites. Nat Commun. 2014 Feb 5;5(1):3216.

64. Higgins GS, Prevo R, Lee YF, Helleday T, Muschel RJ, Taylor S, et al. A Small Interfering RNA Screen of Genes Involved in DNA Repair Identifies Tumor-Specific Radiosensitization by POLQ Knockdown. Cancer Research. 2010 Mar 31;70(7):2984–93.

65. Higgins GS, Boulton SJ. Beyond PARP—POLθ as an anticancer target. Science. 2018 Mar 16;359(6381):1217–8.

66. Polθ inhibitors elicit BRCA-gene synthetic lethality and target PARP inhibitor resistance | Nature Communications [Internet]. [cited 2024 Aug 4]. Available from: https://www.nature.com/articles/s41467-021-23463-8

67. Zatreanu D, Robinson HMR, Alkhatib O, Boursier M, Finch H, Geo L, et al. Polθ inhibitors elicit BRCA-gene synthetic lethality and target PARP inhibitor resistance. Nat Commun. 2021 Jun 17;12(1):3636.

68. Rodriguez-Berriguete G, Ranzani M, Prevo R, Puliyadi R, Machado N, Bolland HR, et al. Small-Molecule Polθ Inhibitors Provide Safe and Effective Tumor Radiosensitization in Preclinical Models. Clinical Cancer Research. 2023 Apr 14;29(8):1631–42.

69. Reece RJ, Maxwell A. DNA gyrase: structure and function. Crit Rev Biochem Mol Biol. 1991;26(3–4):335–75.

70. Zhou J, Gelot C, Pantelidou C, Li A, Yücel H, Davis RE, et al. A first-in-class Polymerase Theta Inhibitor selectively targets Homologous-Recombination-Deficient Tumors. Nat Cancer. 2021 Jun;2(6):598–610.

71. Hall MD, Telma KA, Chang KE, Lee TD, Madigan JP, Lloyd JR, et al. Say no to DMSO: dimethylsulfoxide inactivates cisplatin, carboplatin, and other platinum complexes. Cancer Res. 2014 Jul 15;74(14):3913–22.

72. Scott AD, Waters R. Inducible nucleotide excision repair (NER) of UV-induced cyclobutane pyrimidine dimers in the cell cycle of the budding yeast Saccharomyces cerevisiae: evidence that inducible NER is confined to the G1 phase of the mitotic cell cycle. Mol Gen Genet. 1997 Mar 1;254(1):43–53.

73. Mjelle R, Hegre SA, Aas PA, Slupphaug G, Drabløs F, Sætrom P, et al. Cell cycle regulation of human DNA repair and chromatin remodeling genes. DNA Repair. 2015 Jun 1;30:53–67.

74. Ishibashi A, Saga K, Hisatomi Y, Li Y, Kaneda Y, Nimura K. A simple method using CRISPR-Cas9 to knock-out genes in murine cancerous cell lines. Sci Rep. 2020 Dec 18;10(1):22345.

75. SHLD2 - Shieldin complex subunit 2 - Homo sapiens (Human) | UniProtKB | UniProt [Internet]. [cited 2024 Oct 3]. Available from: https://www.uniprot.org/uniprotkb/Q86V20/entry#sequences

76. Kim JJ, Lee SY, Choi JH, Woo HG, Xhemalce B, Miller KM. PCAF-mediated histone acetylation promotes replication fork degradation by MRE11 and EXO1 in BRCA-deficient cells. Mol Cell. 2020 Oct 15;80(2):327-344.e8.

77. Sessler JL, Hemmi G, Mody TD, Murai T, Burrell A, Young SW. Texaphyrins: Synthesis and Applications. Acc Chem Res. 1994 Feb 1;27(2):43–50.

78. Jalilehvand F, Homayonia S, Zhang P, Ling CC. Gadolinium(III) complex formation with a βcyclodextrin ligand: an XAS study of a potential MRI contrast agent. J Biol Inorg Chem. 2023 Dec 1;28(8):805–11.

79. Preihs C, Arambula JF, Magda D, Jeong H, Yoo D, Cheon J, et al. Recent Developments in Texaphyrin Chemistry and Drug Discovery. Inorg Chem. 2013 Nov 4;52(21):12184–92.

80. Reaney SH, Kwik-Uribe CL, Smith DR. Manganese Oxidation State and Its Implications for Toxicity. Chem Res Toxicol. 2002 Sep 1;15(9):1119–26.

81. Kam WWY, Banati RB. Effects of ionizing radiation on mitochondria. Free Radical Biology and Medicine. 2013 Dec 1;65:607–19.

82. Rouco L, González-Noya AM, Pedrido R, Maneiro M. Pursuing the Elixir of Life: In Vivo Antioxidative Effects of Manganosalen Complexes. Antioxidants (Basel). 2020 Aug 10;9(8):727.

83. Miriyala S, Spasojevic I, Tovmasyan A, Salvemini D, Vujaskovic Z, St. Clair D, et al. Manganese superoxide dismutase, MnSOD and its mimics. Biochim Biophys Acta. 2012 May;1822(5):794–814.

84. Quijano C, Hernandez-Saavedra D, Castro L, McCord JM, Freeman BA, Radi R. Reaction of Peroxynitrite with Mn-Superoxide Dismutase: ROLE OF THE METAL CENTER IN DECOMPOSITION KINETICS AND NITRATION*. Journal of Biological Chemistry. 2001 Apr 13;276(15):11631–8.

85. Gauter-Fleckenstein B, Reboucas JS, Fleckenstein K, Tovmasyan A, Owzar K, Jiang C, et al. Robust rat pulmonary radioprotection by a lipophilic Mn N-alkylpyridylporphyrin, MnTnHex-2PyP5+. Redox Biol. 2014 Jan 9;2:400–10.

86. Marsh JW, Hacker L, Huang S, Boulet MHC, White JRG, Martin LAW, et al. Fluorogenic platinum(IV) complexes as potential predictors for the design of hypoxia-activated platinum(IV) prodrugs. Dalton Trans. 2024 Sep 10;53(35):14811–6.

87. Johnstone TC, Suntharalingam K, Lippard SJ. The Next Generation of Platinum Drugs: Targeted Pt(II) Agents, Nanoparticle Delivery, and Pt(IV) Prodrugs. Chem Rev. 2016 Mar 9;116(5):3436–86.

88. Thiabaud G, Arambula JF, Siddik ZH, Sessler JL. Photoinduced Reduction of PtIV within an Anti-Proliferative PtIV–Texaphyrin Conjugate. Chemistry – A European Journal. 2014;20(29):8942–7.

89. Gibson D. Platinum(IV) anticancer agents; are we en route to the holy grail or to a dead end? Journal of Inorganic Biochemistry. 2021 Apr 1;217:111353.

90. Koltai T, Reshkin SJ, Harguindey S. Chapter 16 - Pharmacological interventions part IV: Metabolic modifiers. In: Koltai T, Reshkin SJ, Harguindey S, editors. An Innovative Approach to Understanding and Treating Cancer: Targeting pH [Internet]. Academic Press; 2020 [cited 2024 Oct 3]. p. 361–416. Available from: https://www.sciencedirect.com/science/article/pii/B9780128190593000162

91. Kankotia S, Stacpoole PW. Dichloroacetate and cancer: New home for an orphan drug? Biochimica et Biophysica Acta (BBA) - Reviews on Cancer. 2014 Dec 1;1846(2):617–29.

92. Xue X, You S, Zhang Q, Wu Y, Zou G zhang, Wang PC, et al. Mitaplatin Increases Sensitivity of Tumor Cells to Cisplatin by Inducing Mitochondrial Dysfunction. Mol Pharmaceutics. 2012 Mar 5;9(3):634–44.

93. Anand R, Ranjha L, Cannavo E, Cejka P. Phosphorylated CtIP Functions as a Co-factor of the MRE11-RAD50-NBS1 Endonuclease in DNA End Resection. Mol Cell. 2016 Dec 1;64(5):940–50.

94. Tomimatsu N, Mukherjee B, Deland K, Kurimasa A, Bolderson E, Khanna KK, et al. Exo1 plays a major role in DNA end resection in humans and influences double-strand break repair and damage signaling decisions. DNA Repair (Amst). 2012 Apr 1;11(4):441–8.

95. Yi G, Sung Y, Kim C, Ra JS, Hirakawa H, Kato TA, et al. DNA polymerase θ-mediated repair of high LET radiation-induced complex DNA double-strand breaks. Nucleic Acids Research. 2023 Mar 21;51(5):2257–69.

96. Schrempf A, Slyskova J, Loizou JI. Targeting the DNA Repair Enzyme Polymerase θ in Cancer Therapy. Trends in Cancer. 2021 Feb 1;7(2):98–111.

97. Kruchinin AA, Makarova AV. Multifaceted Nature of DNA Polymerase θ. International Journal of Molecular Sciences. 2023 Jan;24(4):3619.

98. Seki M, Masutani C, Yang LW, Schuffert A, Iwai S, Bahar I, et al. High-efficiency bypass of DNA damage by human DNA polymerase Q. The EMBO Journal. 2004 Nov 10;23(22):4484–94.

99. Yoon JH, Johnson RE, Prakash L, Prakash S. Genetic evidence for reconfiguration of DNA polymerase θ active site for error-free translesion synthesis in human cells. Journal of Biological Chemistry. 2020 May 1;295(18):5918–27.

100. Hogg M, Seki M, Wood RD, Doublié S, Wallace SS. Lesion bypass activity of DNA polymerase θ (POLQ) is an intrinsic property of the pol domain and depends on unique sequence inserts. J Mol Biol. 2011 Jan 21;405(3):642–52.

101. Bukowska B, Karwowski BT. The Clustered DNA Lesions - Types, Pathways of Repair and Relevance to Human Health. Curr Med Chem. 2018;25(23):2722–35.

102. Sage E, Shikazono N. Radiation-induced clustered DNA lesions: Repair and mutagenesis. Free Radical Biology and Medicine. 2017 Jun 1;107:125–35.

103. Bellon S, Shikazono N, Cunniffe S, Lomax M, O'Neill P. Processing of thymine glycol in a clustered DNA damage site: mutagenic or cytotoxic. Nucleic Acids Res. 2009 Jul;37(13):4430–40.